Dear Author,

Here are the proofs of your article.

- You can submit your corrections **online**, via **e-mail** or by **fax**.
- For **online** submission please insert your corrections in the online correction form. Always indicate the line number to which the correction refers.
- You can also insert your corrections in the proof PDF and **email** the annotated PDF.
- For fax submission, please ensure that your corrections are clearly legible. Use a fine black pen and write the correction in the margin, not too close to the edge of the page.
- Remember to note the **journal title**, **article number**, and **your name** when sending your response via e-mail or fax.
- **Check** the metadata sheet to make sure that the header information, especially author names and the corresponding affiliations are correctly shown.
- **Check** the questions that may have arisen during copy editing and insert your answers/ corrections.
- **Check** that the text is complete and that all figures, tables and their legends are included. Also check the accuracy of special characters, equations, and electronic supplementary material if applicable. If necessary refer to the *Edited manuscript*.
- The publication of inaccurate data such as dosages and units can have serious consequences. Please take particular care that all such details are correct.
- Please **do not** make changes that involve only matters of style. We have generally introduced forms that follow the journal's style.
  Substantial changes in content, e.g., new results, corrected values, title and authorship are not allowed without the approval of the responsible editor. In such a case, please contact the Editorial Office and return his/her consent together with the proof.
- If we do not receive your corrections **within 48 hours**, we will send you a reminder.
- Your article will be published **Online First** approximately one week after receipt of your corrected proofs. This is the **official first publication** citable with the DOI. **Further changes are, therefore, not possible.**
- The **printed version** will follow in a forthcoming issue.

Please note

After online publication, subscribers (personal/institutional) to this journal will have access to the complete article via the DOI using the URL: http://dx.doi.org/[DOI].
If you would like to know when your article has been published online, take advantage of our free alert service. For registration and further information go to: http://www.link.springer.com.

Due to the electronic nature of the procedure, the manuscript and the original figures will only be returned to you on special request. When you return your corrections, please inform us if you would like to have these documents returned.

Metadata of the article that will be visualized in OnlineFirst

ArticleTitle	Evidence of a new geothermal prospect in the Northern-Central trans-Mexican volcanic belt: Rancho Nuevo, Guanajuato, Mexico	
Article Sub-Title		
Article CopyRight	Universidad Complutense de Madrid (This will be the copyright line in the final PDF)	
Journal Name	Journal of Iberian Geology	
Corresponding Author	Family Name	**Landa-Arreguín**
	Particle	
	Given Name	**J. F. A.**
	Suffix	
	Division	
	Organization	Posgrado en Ciencias de La Tierra, Universidad Nacional Autónoma de México
	Address	Del. Coyoacán, 04510, Ciudad de México, México
	Phone	
	Fax	
	Email	jorgefl@igeofisica.unam.mx
	URL	
	ORCID	http://orcid.org/0000-0003-4855-075X
Author	Family Name	**Villanueva-Estrada**
	Particle	
	Given Name	**R. E.**
	Suffix	
	Division	Instituto de Geofísica
	Organization	Universidad Nacional Autónoma de México
	Address	Unidad Michoacán Antigua Carretera a Pátzcuaro 8701, Residencial San José de La Huerta, 58341, Morelia, Mich., Mexico
	Phone	
	Fax	
	Email	
	URL	
	ORCID	
Author	Family Name	**Rodríguez-Díaz**
	Particle	
	Given Name	**A. A.**
	Suffix	
	Division	Instituto de Geofísica
	Organization	Universidad Nacional Autónoma de México
	Address	Ciudad Universitaria, 04510, Ciudad de Mexico, Mexico
	Phone	
	Fax	

	Email	
	URL	
	ORCID	
Author	Family Name	**Morales-Arredondo**
	Particle	
	Given Name	**J. I.**
	Suffix	
	Division	Instituto de Geofísica
	Organization	Universidad Nacional Autónoma de México
	Address	Ciudad Universitaria, 04510, Ciudad de Mexico, Mexico
	Phone	
	Fax	
	Email	
	URL	
	ORCID	
Author	Family Name	**Miller**
	Particle	
	Given Name	**R. Rocha**
	Suffix	
	Division	Instituto de Geofísica
	Organization	Universidad Nacional Autónoma de México
	Address	Ciudad Universitaria, 04510, Ciudad de Mexico, Mexico
	Phone	
	Fax	
	Email	
	URL	
	ORCID	
Author	Family Name	**Alfonso**
	Particle	
	Given Name	**P.**
	Suffix	
	Division	Departament d'Enginyeria Minera I Recursos Naturals
	Organization	Universitat Politècnica de Catalunya
	Address	Av. Bases de Manresa 61−73, 08242, Manresa, Spain
	Phone	
	Fax	
	Email	
	URL	
	ORCID	

Schedule	Received	25 August 2020
	Revised	
	Accepted	20 July 2021

Abstract

Thermal manifestations are commonly found in central Mexico as result of the volcanic activity originating from the formation of the Trans-Mexican Volcanic Belt during the Quaternary. The Rancho Nuevo hot spring is one of them that has not been described before with a discharge temperature near 92 °C. The goal

of the present study is to provide geothermal characteristics of thermal manifestations at Rancho Nuevo location based on geochemical and mineralogical results to explain deep-subsurface processes that occurred in the geothermal system. The presence of kaolinite, montmorillonite, opal, zeolite, barite, pyrite, and stibnite in altered soil sediments or around the hot springs identified by the techniques used in the present study, confirms the presence of hydrothermal activity. In addition, based on the X-ray diffraction, calcite precipitates at the surface of the thermal springs. This mineral association reflects deep geothermal processes and is eventually deposited in shallow zones. Fluid mixing processes and variations in redox conditions are suggested by mineral association and isotopic sulfur data. Finally, based on the physicochemical data provided by the water samples and the discharge conditions of the springs, stability diagrams were constructed for pyrite, barite, and zeolites using the Geochemist's Work Bench program to corroborate these data with the mineralogical results. The mineralogical results and distribution and N-S trend of mineral associations suggest interaction processes between geothermal fluid and rocks of the stratigraphic sequence, and active major faults, enabling the upward flow of deep geothermal fluids. The approach to the conceptual model of the Rancho Nuevo geothermal prospect reveals an attractive potential for the exploration of a viable geothermal resource in central Mexico.

Resumen	En el centro de México es común encontrar manifestaciones termales como resultado de la actividad volcánica que originó la formación del Cinturón Volcánico Trans-Mexicano durante el Cuaternario. El manantial caliente de Rancho Nuevo es una de ellas el cual no ha sido descrita antes cuya temperatura de descarga es de aproximadamente 92 °C. El objetivo del presente estudio es proporcionar las características geotérmicas de las manifestaciones termales localizadas en el poblado de Rancho Nuevo, considerando los resultados geoquímicos y mineralógicos, para explicar los procesos ocurridos a profundidad en el sistema geotérmico. La presencia de caolinita, montmorillonita, ópalo, zeolita, barita, pirita y estibinita identificadas por las técnicas utilizadas, tanto en sedimentos del suelo como alrededor de las fuentes termales, confirma la presencia de actividad hidrotermal. Además, de acuerdo a los resultados de difracción de rayos X, la calcita precipita en la superficie de las fuentes termales. Esta asociación mineral refleja procesos geotérmicos profundos y finalmente es depositada en zonas poco profundas. Los procesos de mezcla de fluidos y las variaciones en las condiciones redox son sugeridas por la asociación mineral y los datos de azufre isotópico. Finalmente, con base a los datos fisicoquímicos proporcionados por las muestras de agua y las condiciones de descarga de los manantiales, se construyeron diagramas de estabilidad para pirita, barita y zeolita para corroborar estos datos con los resultados mineralógicos. Los resultados mineralógicos y su distribución, así como la tendencia N-S de las asociaciones minerales, sugieren procesos de interacción entre el fluido geotérmico y las rocas de la secuencia estratigráfica, y fallas mayores activas, que permiten el flujo ascendente de fluidos profundos. El enfoque del modelo conceptual del prospecto geotérmico Rancho Nuevo revela un potencial atractivo para la exploración de un recurso geotérmico viable en el centro de México.
Keywords (separated by '-')	Geothermal potential - Rancho Nuevo geothermal prospect - Hot spring mineralization - Deep-subsurface processes
Palabras clave (separated by '-')	Potencial geotérmico - Prospecto geotérmico de Rancho Nuevo - Mineralización de manantial caliente - Procesos profundos-subsuperficiales
Footnote Information	

Journal of Iberian Geology
https://doi.org/10.1007/s41513-021-00173-0

REVIEW ARTICLE

Evidence of a new geothermal prospect in the Northern-Central trans-Mexican volcanic belt: Rancho Nuevo, Guanajuato, Mexico

J. F. A. Landa-Arreguín[1] · R. E. Villanueva-Estrada[2] · A. A. Rodríguez-Díaz[3] · J. I. Morales-Arredondo[3] · R. Rocha Miller[3] · P. Alfonso[4]

Received: 25 August 2020 / Accepted: 20 July 2021

Abstract

Thermal manifestations are commonly found in central Mexico as result of the volcanic activity originating from the formation of the Trans-Mexican Volcanic Belt during the Quaternary. The Rancho Nuevo hot spring is one of them that has not been described before with a discharge temperature near 92 °C. The goal of the present study is to provide geothermal characteristics of thermal manifestations at Rancho Nuevo location based on geochemical and mineralogical results to explain deep-subsurface processes that occurred in the geothermal system. The presence of kaolinite, montmorillonite, opal, zeolite, barite, pyrite, and stibnite in altered soil sediments or around the hot springs identified by the techniques used in the present study, confirms the presence of hydrothermal activity. In addition, based on the X-ray diffraction, calcite precipitates at the surface of the thermal springs. This mineral association reflects deep geothermal processes and is eventually deposited in shallow zones. Fluid mixing processes and variations in redox conditions are suggested by mineral association and isotopic sulfur data. Finally, based on the physicochemical data provided by the water samples and the discharge conditions of the springs, stability diagrams were constructed for pyrite, barite, and zeolites using the Geochemist's Work Bench program to corroborate these data with the mineralogical results. The mineralogical results and distribution and N-S trend of mineral associations suggest interaction processes between geothermal fluid and rocks of the stratigraphic sequence, and active major faults, enabling the upward flow of deep geothermal fluids. The approach to the conceptual model of the Rancho Nuevo geothermal prospect reveals an attractive potential for the exploration of a viable geothermal resource in central Mexico.

Keywords Geothermal potential · Rancho Nuevo geothermal prospect · Hot spring mineralization · Deep-subsurface processes

Resumen

En el centro de México es común encontrar manifestaciones termales como resultado de la actividad volcánica que originó la formación del Cinturón Volcánico Trans-Mexicano durante el Cuaternario. El manantial caliente de Rancho Nuevo es

✉ J. F. A. Landa-Arreguín
jorgefl@igeofisica.unam.mx

[1] Posgrado en Ciencias de La Tierra, Universidad Nacional Autónoma de México, Del. Coyoacán, 04510 Ciudad de México, México

[2] Instituto de Geofísica, Universidad Nacional Autónoma de México, Unidad Michoacán Antigua Carretera a Pátzcuaro 8701, Residencial San José de La Huerta, 58341 Morelia, Mich., Mexico

[3] Instituto de Geofísica, Universidad Nacional Autónoma de México, Ciudad Universitaria, 04510 Ciudad de Mexico, Mexico

[4] Departament d'Enginyeria Minera I Recursos Naturals, Universitat Politècnica de Catalunya, Av. Bases de Manresa 61–73, 08242 Manresa, Spain

una de ellas el cual no ha sido descrita antes cuya temperatura de descarga es de aproximadamente 92 °C. El objetivo del presente estudio es proporcionar las características geotérmicas de las manifestaciones termales localizadas en el poblado de Rancho Nuevo, considerando los resultados geoquímicos y mineralógicos, para explicar los procesos ocurridos a profundidad en el sistema geotérmico. La presencia de caolinita, montmorillonita, ópalo, zeolita, barita, pirita y estibinita identificadas por las técnicas utilizadas, tanto en sedimentos del suelo como alrededor de las fuentes termales, confirma la presencia de actividad hidrotermal. Además, de acuerdo a los resultados de difracción de rayos X, la calcita precipita en la superficie de las fuentes termales. Esta asociación mineral refleja procesos geotérmicos profundos y finalmente es depositada en zonas poco profundas. Los procesos de mezcla de fluidos y las variaciones en las condiciones redox son sugeridas por la asociación mineral y los datos de azufre isotópico. Finalmente, con base a los datos fisicoquímicos proporcionados por las muestras de agua y las condiciones de descarga de los manantiales, se construyeron diagramas de estabilidad para pirita, barita y zeolita para corroborar estos datos con los resultados mineralógicos. Los resultados mineralógicos y su distribución, así como la tendencia N-S de las asociaciones minerales, sugieren procesos de interacción entre el fluido geotérmico y las rocas de la secuencia estratigráfica, y fallas mayores activas, que permiten el flujo ascendente de fluidos profundos. El enfoque del modelo conceptual del prospecto geotérmico Rancho Nuevo revela un potencial atractivo para la exploración de un recurso geotérmico viable en el centro de México.

Palabras clave Potencial geotérmico · Prospecto geotérmico de Rancho Nuevo · Mineralización de manantial caliente · Procesos profundos-subsuperficiales

1 Introduction

Mineral alterations as a result of water–rock interaction processes at depth provide evidence of the evolution of hydrothermal systems. In particular, mineral associations and their distribution provide information about the main characteristics of hydrothermal reservoirs and fluids, including their (a) temperature and acidity (Browne, 1970; Elders et al., 2014), (b) formation equilibrium conditions (Ármansson, 2009; Henley & Ellis, 1983), and (c) permeability (Browne, 1970; Canet et al., 2015). Besides, alteration mineral associations can be used for classifying geothermal systems (Ronoh, 2015). Therefore, the study of alteration minerals is one of the most important geological means of defining the conditions of hydrothermal reservoirs and fluids during the exploration of geothermal systems (e.g., Canet et al., , 2015, 2019; Reyes, 1990).

The geological province known as the Trans-Mexican Volcanic Belt (TMVB) extending across central Mexico (Fig. 1) is an active volcanic arc. This province has undergone extensive events since the Late Miocene which are shown in a large variation in the composition of volcanic rocks and volcanic style, and an intra-arc extensional tectonics (Alaniz-Álvarez & Nieto-Samaniego, 2007; Ferrari et al., 2012; Gómez-Tuena et al., 2007; Verma et al., 2016). These characteristics generated favorable geological conditions for the formation of geothermal systems (plays) of volcanic and intrusive type or extensional domain (e.g. Moeck, 2014), with a strong influence of regional extensional processes (e.g. Gutiérrez-Negrín, 2015). Therefore, the geological environment of the TMVB and its high heat flow (~ 80/200 mW/m^2) has favored the formation of geothermal fields and promising geothermal prospects (Prol-Ledesma et al., 2018), such as Humeros Caldera (Juárez-Arriaga et al., 2018; Carrasco-Núñez et al., 2017), and Acoculco Caldera (Sosa-Ceballos et al., 2018) eastern TMVB, Los Azufres Caldera (Arce et al., 2012) and San Bartolomé de Los Baños (Canet et al., 2019) central TMVB, and La Primavera Caldera (Bolós et al., 2019) western TMVB. The Trans-Mexican Volcanic Belt contains numerous thermal manifestations whose mineral associations and distributions indicate the occurrence of hydrothermal processes related to magmatic activity and extensive fault systems (e.g., Canet et al., 2019; Pérez-Martínez et al., 2020; Torres-Alvarado, 2000; Torres-Alvarado et al., 2007). In that geological province, the study of alteration minerals has been a useful tool for characterizing and understanding the potential of several high-temperature geothermal fields, such as Los Azufres, Michoacán (Molina-Martínez, 2013), and Los Humeros, Puebla (Elders et al., 2014). Despite the current geothermal interest in the TMVB, few studies have explored new geothermal prospects, and such is the case for the Geothermal Zone of Rancho Nuevo (GZRN) located along the central edge of the province, whose prominent thermal activity, characterized by thermal wells and two hot springs, has not yet been studied even. Hence the area represents a suitable area for geothermal exploration.

Therefore, the goal of the present study is to define the geothermal characteristics of thermal manifestations at the GZRN based on mineralogical evidence obtained from various techniques that help to explain their geochemical processes. Soil sediments and water samples for mineralogical and hydrogeochemistry studies respectively were taken in August 2016 (rainy season) and March 2017 (dry season) of the Rancho Nuevo (GRN) hot spring and the Los Mezquites (GHM) hot spring. The information generated from this

Journal : Large 41513 | Article No : 173 | Pages : 20 | MS Code : 173 | Dispatch : 24-7-2021

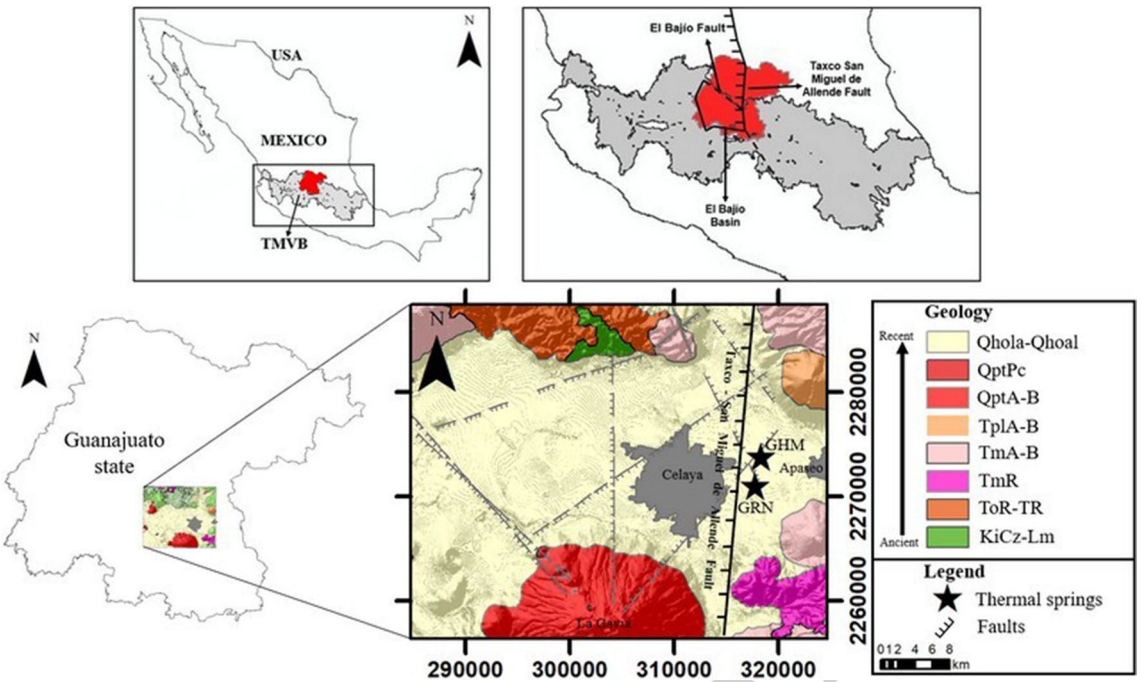

Fig. 1 Map shows the location of the TMVB, the Taxco-San Miguel de Allende fault and the El Bajío basin delimited by two important faults, as well as the local geology and the location of the GRN and GHM hot springs

study and its interpretation is useful for characterizing or classifying a system based on its mineralogy. In addition, a complementary geochemical study of the fluids in the geothermal system was carried out.

2 Geological setting

The GZRN is located southeast of the state of Guanajuato between the municipalities of Celaya and Apaseo el Grande on the central edge of the TMVB where there are several thermal wells and two hot springs defined as GRN and GHM (Landa-Arreguín et al., 2017; Pita-de la Paz et al., 2016) (Fig. 1).

The TMVB is a physiographic province located in center of Mexico and it is considered a volcanic arc built on the southern edge of the North America plate and formed by the subduction of the Rivera and Cocos plates (Ferrari et al., 2012). The igneous activity of the TMVB has undergone significant changes in the geographical location throughout its geological history and in its volcanic style, thus in its chemical composition (Gómez-Tuena et al., 2005). This physiographic province also presents another particular feature such as a significant variation in the arc width and a slight obliquity with respect to the trench (Ferrari et al., 2012). During the formation of the TMVB, there was an extensional period with intense magmatism controlled by the regional fault systems (NE-SW, NW–SE, E-W, and N-S; Alaniz-Álvarez & Nieto-Samaniego, 2005; Garduño-Monroy et al., 1993; Rosas-Elguera & Urrutia-Fucugauchi, 1998). The TMVB is represented by more than 8,000 structures represented by stratovolcanoes, monogenetic volcanoes, calderas, some intrusive bodies (Demant, 1978; Gómez-Tuena et al., 2005) and where the Los Humeros, Los Azufres, Domo San Pedro geothermal fields and many hot springs, all of them formed by volcanic activity, are emplaced. Therefore, in the whole of the TMVB has an important geothermal potential, but few studies of the area have been done so far, except for the areas where geothermal fields are located. The TMVB is distributed along ~ 1,000 km, with a variable amplitude between 80 and 230 km (Gómez-Tuena et al., 2005) and currently emplaced in pre-existing, active tectonic basins (Campos-Enriquez and Sánchez-Zamora 2000; Venegas-Salgado et al., 1985). The study area is located in one of these basins known as El Bajío, a semi-graben delimited by the El Bajío and Taxco-San Miguel de Allende regional faults (Botero-Santa et al., 2015).

The oldest lithological unit in the region, defined as the basement, emerges to the north of the GZRN. It is defined by Cretaceous volcano-sedimentary rocks and the clay-calcareous rocks (KiCz-Lm) of the Soyatal Formation (Cerca-Martínez et al., 2000). Units of rhyolitic lavas and tuff rhyolite of the Oligocene age were also identified in the area (ToR). The Oligocene unit is unconformable and overlain by well-consolidated and breached ignimbrites (TR) with intercalations of pyroclastic deposits of the Miocene-Pliocene

Journal : Large 41513 | Article No : 173 | Pages : 20 | MS Code : 173 | Dispatch : 24-7-2021

age. Overlying these units are two pyroclastic and volcanic units: (a) Huapango Ignimbrite (TmR) with a radiometric age of 5.3 Ma (Aguirre-Díaz & López-Martínez, 2001, 2003) and (b) a sequence composed of alternating lava flows of andesitic and basalt composition (TmA-B) and andesitic pyroclastic deposits of the Pliocene age (TplA-B) (Aguirre-Díaz & López-Martínez, 2003; Nieto-Samaniego et al., 1999).

The youngest units are located south and west of the hot springs. They comprise andesitic-basaltic lavas (QptA-B) produced by eruptions of the Llano Grande and La Gavia volcanoes (Nieto-Samaniego et al., 1999) associated with the Michoacán-Guanajuato Volcanic Field (Aguirre-Díaz & López-Martínez, 2003). According to dating and paleomagnetic data, the age of these events is from 1.3 to 0.83 Ma (CEAG, 2000). A lacustrine sequence of the Pliocene–Pleistocene-Holocene (Qhola) composed of alternating pyroclastic conglomerates and sandstone sediments, as well as fine sediment units *ca*. 100 m thick (Nieto-Samaniego et al., 1999), hosts the hot springs examined in the present study (Fig. 1). Alluvial deposits (Qhoal) are also widely distributed throughout the study area.

3 Hydrothermal activity

In different municipalities of Guanajuato such as Juventino Rosas, Celaya and Villagrán located west near to the study area, thermal activity was reported in lots of wells being another proof of that activity in the region (Morales-Arredondo et al., 2015; Landa-Arreguín et al., 2017; Ortega-Gutiérrez et al., 2019, respectively), in addition to the surface evidence characterized by GRN and GHM hot springs. The GRN hot spring has a diameter of *ca.* 4 m. It may be characterized as a hydrothermal manifestation with liquid and gas emanations and discharge temperatures that can reach 92 °C. The thermal water discharges into a channel connected with a hot spring (Fig. 2a). In the surroundings, there is also a fossil mud pool and depressions of paleo-springs with white crust formation on the periphery and irregular activity, since they may flood in the rainy season yet contain no water in the dry season (Fig. 2b, c). In areas of continuous venting and bubbling around the GRN hot spring, there are sediments coated with orange-yellow and greenish biofilms. The GHM hot spring is located north of the main manifestation in a ranch called "Los Mezquites" whose discharge temperature is around 32 °C whose diameter is *ca*. 4 m. At the beginning of the last century, the thermal springs of the Hacienda Los Mezquites were used as recreational and medicinal baths (Fig. 2e). Currently, there is only one main spring, and the spa is inactive (Fig. 2d). Moreover, about 30 km east of the Rancho Nuevo location is located San Bartolomé de los Baños, another thermal site where the oldest record of thermal activity (colonial period) in the area within the El Bajío basin is known (Arredondo, 2012). Therefore, this region is considered an important hydrothermal zone located in the TMVB and where there are few studies about geothermal exploration.

4 Materials and methods

4.1 Sampling

To compare and analyze the physicochemical parameters of thermal water in two different seasons, two sampling campaigns were carried out in August 2016 (rainy season) and March 2017 (dry season). In the first sampling campaign, sediment samples were collected at sites near the springs at a depth of 10 cm; the surface material, including the organic matter, was removed before excavating the sample. Fossil and mud pool samples were taken some meters near to the GRN hot spring. Water samples of the springs were also taken in high-density polyethylene bottles, washed before use with 1 N HNO_3 and then with Milli-Q water, according to Mexican official standard (NOM-014-SSA1-1993). The water samples were filtered using 0.45 µm cellulose membrane, acidified by adding ultrapure HNO_3 until reaching a pH of 2 and retained at 5 °C for their conservation prior analysis. The field parameters of the thermal water were measured, including the discharge temperature, electrical conductivity (EC), total dissolved solids (TDS), and pH (Table 1). A multiparameter device (model MM150, trademark sensION) employing measurement techniques previously validated by the Standard Methods for the Examination of Water and Wastewater (1995) was used. The device was calibrated in the field with standard solutions of pH and EC before taking samples. The concentrations of silica and sulfide were also determined in the field using a colorimeter (model DR900, HACH). The silica concentration was assessed by the 4500-SiO_2 SILICA (2017) molybdosilicate method and the sulfide concentration by the 4500-S^{2-} SULFIDE (2017) methylene blue method. The bicarbonate concentration was measured by the acid titration method using an automatic titrator (Metrohm model, Tritanto 905). Ionic charge balance was calculated, and the results were < 5%; therefore, they are considered very reliable (Rouwet, 2006; Taran et al., 1998;). The second field campaign, random samples of wet sediments were collected from the interior periphery of the GRN hot spring to identify the mineralogical phases of the sediments interacting with the thermal water of the hot spring.

To identify greater diversity of alteration minerals in soil sediments of coarse grain (> 0.074 mm) and fine grain fraction (< 0.074 mm) sizes of both hot springs, different techniques were used. Minerals of non-consolidated material and without prior separation were identified by stereoscopic

Journal : Large 41513 | Article No : 173 | Pages : 20 | MS Code : 173 | Dispatch : 24-7-2021

Fig. 2 Photographs of the hot springs: **a** The GRN hot spring whose diameter is ~ 4 m and the discharge temperature of ~ 92 °C; it is evident the gas emanation. Stars indicate sites where samples were taken for mineralogical analysis into the GRN hot spring. **b** The fossil mud pool in the rainy season located some meters of distance from GRN hot spring and whose diameter is ~ 1 m. **c** The same fossil mud pool in the dry season. **d** Hacienda Los Mezquites contains the old thermal baths in the study area (1900). **e** The GHM hot spring whose diameter is ~ 4 m and the discharge temperature of ~ 32 °C

microscopy, short-wave infrared (SWIR), environmental scanning electron microscopy (ESEM), and by electron probe microanalyzer (EPMA). Some clay minerals, such as illite and kaolinite, are common alteration minerals of hydrothermal systems, their formation is evidence of specific conditions therefore, to identify and classify the minerals of fine fraction with prior separation X-ray diffraction (XRD) analysis was used.

4.2 Microscopy analysis

To identify some alteration minerals of soil sediment samples an Olympus SZX-9 stereoscopic microscope was used. The observations of soil sediments samples of both hot springs without prior treatment or separation were carried out at the Laboratory of Petrography and Microthermometry (Laboratorio de Petrografía y Microtermometría) of the Geophysics Institute of the National Autonomous University of Mexico (Universidad Nacional Autónoma de México [UNAM]). Thin sections of non-consolidated material in the soil sediment samples from the hot springs were prepared, critical point-dried, and coated with a thin layer of carbon in order to identify the alteration minerals in coarse fraction. First, ESEM was used for the coarse soil sediment fractions at the Laboratory of Petrography and Microthermometry of the Geophysics Institute of UNAM. Then, an electron probe microanalyzer (EPMA; model JXA-8900 XR, JEOL) was used for identifying alteration minerals in fine soil sediment fractions at the University Laboratory of Petrology (Laboratorio Universitario de

Journal : Large 41513 | Article No : 173 | Pages : 20 | MS Code : 173 | Dispatch : 24-7-2021

Table 1 Field parameters and chemical concentrations of water samples collected in August 2016 andF March 2017

Season	LD	Temp (°C)	pH	Eh (V)	EC (µS/cm)	TDS	S^{2-} (mg/L)	SiO_2	Na^+ 0.1098	K^+ 0.1226	Ca^{2+} 0.0798	Mg^{2+} 0.0005	HCO_3^- * (mg/L)	SO_4^{2-} 0.8078	Cl^- 0.0923	F^- 0.465	Ba 0.117	As 0.132	Al 8.132 (µg/L)	Fe 1.596
Rainy	GRN-16	92	8.3	-0.38	1189	785	0.7	72	420	39.1	0.8	0.02	506	127	280	13.9	63	634	247	14
Dry	GRN-17	90	8.4	-0.38	1940	1241	0.4	158	479	52.3	11.1	0.02	480	173	374	15.9	38	296	141	5
Rainy	GHM-16	32	7.2	-0.22	1382	913	0.1	35	474	38.5	21.5	1.2	717	113	275	11.7	209	681	11	380
Dry	GHM-17	25	7.1	-0.21	1965	1258	0.2	115	382	45.9	43.5	0.9	743	43	289	8.1	190	330	18	11

LD Limit of detection
*Undetermined

Petrología [LUP]) that belongs at the National Laboratory of Geochemistry and Mineralogy (Laboratorio Nacional de Geoquímica y Mineralogía [LANGEM]) of the Geophysics Institute of UNAM. The electron probe enabled back-scattered electrons (BSE) images to be obtained and X-ray energy dispersive spectroscopy (EDS) qualitative analyses to be carried out.

4.3 Short-wave infrared

Sediment soil samples from the GRN and GHM hot springs, and from the fossil mud pool were analyzed at the Laboratory of Petrography and Microthermometry of the Geophysics Institute of UNAM by a portal LabSpec Pro spectrophotometer (Analytical Spectral Devices Inc.). The reflectance was measured on dry surfaces without prior sample treatment. The range of selected wavelengths was 1300 to 2500 nm, corresponding with the SWIR region spectrum. The sampling interval was 2 nm every 0.1 s. An internal radiation source and optical detector were used. The identification of the minerals was carried out manually by comparing the position and shape of the absorption features with spectra tables (Clark et al., 2007; Spectral International Inc., 1994).

4.4 X-ray diffraction

The x-ray diffraction (XRD) technique was used to identify the bulk mineralogy of the mineralized sediments of fine fraction (< 0.074 mm) of both hot springs, the sediments interacting with the thermal water of the GRN hot spring and the white crust formation of the fossil mud pool. First, the samples were crushed, homogenized with an agate mortar, and sieved to a mesh size of 0.074 mm. The mineral composition was determined using an EMPYREAN diffractometer equipped with a nickel filter, a fine-focus copper tube, and a PIXcel3D detector operating at 40 mA and 45 kV at the National Laboratory of Geochemistry and Mineralogy (Laboratorio Nacional de Geoquímica y Mineralogía [LANGEM]) of the Geology Institute of UNAM. The crushed samples were mounted on back-side aluminum holders. The step-scan method was selected: Measurements were made at a 2θ angular interval from 5–70° with an integration time of 40 s and a step size of 0.003°. The oriented fraction method was used to identify clay minerals. Samples were saturated with ethylene glycol and heated to 550 °C (to identify kaolinite in particular) (Moore & Reynolds, 1997). Phase identification was performed using the PDF-2 and ICSD databases. The semiquantitative results were based on the intensity of the corundum peak as a standard for the relative intensity ratio (RIR; Hillier, 2000).

Journal : Large 41513 | Article No : 173 | Pages : 20 | MS Code : 173 | Dispatch : 24-7-2021

4.5 Chemical analysis of thermal water

All the water samples were filtered in the field. The analysis of major cations (Na^+, K^+, Li^+, Ca^{2+}, Mg^{2+}) and some trace elements (Ba, As, Al, Fe) concentrations are used to built-up the stability diagrams. An ionic chromatography system (Dionex/5000, Thermo Scientific) was used to analyze the ionic concentration of thermal waters at the Geothermal Fluids Geochemical Laboratory of the Geophysics Institute of UNAM. The analysis of major anions (Cl^-, SO_4^{2-}, F^-) was made using a Dionex Ion Pac AS11-HC column (4 × 250 mm) with a mobile phase of NaOH 30 mM was used; to analyze the cations, a Dionex Ion Pac CS11-HC column (4 × 250 mm) with a mobile phase of methanesulfonic acid mM. For both analyses, high purity standards of each ion were used under the criterion that the coefficient variation is ≤ 2.0% of the reference standard for the calibration curves. The ion balance (IB) was also performed; both water samples had an IB < 5%. To analyze the trace elements, induced coupled plasma mass spectrometry (ICP-MS) was performed with an ICP mass spectrometer (iCAP Qc, Thermo Scientific) at the ICP-MS Laboratory of the Geophysics Institute of UNAM. The ICP mass spectrometer was previously optimized for sample analysis with a certified aqueous solution suitable for a wide range of masses (Li, Co, In, Ba, Bi, Ce, and U of 1 µg/L). The calibration curve was prepared from a multi-elemental stock solution (QCS-26) and was calculated for 16 concentrations (0, 0.1, 0.25, 0.5, 0.75, 1, 2.5, 5, 7.5, 10, 25, 50, 100, 250, and 500 µg/L). The instrumental drift was corrected with an Indium internal standard (10 µg/L). The limit of detection was 0.117 µg/L for Ba, 0.132 µg/L for As, and 8.1323 µg/L for Al.

4.6 Sulfur isotopes

Sulfur isotopes (^{34}S) were measured in the authigenic barite and pyrite of soil sediments and pyrite and stibnite of the fossil mud pool. A Wilfley shaking table was used to concentrate dense metal minerals, especially sulfides and barite. Thirty-five kilograms of samples were concentrated. Then, the barite, pyrite, and stibnite were separated from the concentrated sample of each sampling campaign by handpicking using the same Olympus SZX-9 stereoscopic microscope with a 40 × magnification lens. The purity of the samples was tested by examination with a binocular microscope.

The barite and pyrite from soils from both hot springs, and the stibnite and pyrite from the fossil mud pool were the only minerals obtained from the separation process. Each sample was introduced into tin capsules that formed balls ready to be analyzed. Pyrite, stibnite, and barite were obtained by scratching the surface of polished samples, avoiding contamination. Sulfur isotope analyses were carried out at the Scientific and Technological Centers (Centres Científics i Tecnològics [CCiT]) of the University of Barcelona using a continuous flow isotope-ratio mass spectrometer (Delta Plus XP, Thermo Fisher) coupled with an elemental analyzer (TC-EA; Carlo Erba 1108) according to the method of Giesemann et al. (1994). Results are expressed in ‰ relative to the V-CDT standard. Analytical precision is within ± 0.2 ‰ (1 SD).

4.7 Phase diagrams

The phase diagrams were made from the chemical composition of the water (Table 1) of the hot spring samples. The chemical results were inputted into a database made in the GSS module (Geochemist's Spreadsheets) of the Geochemist's Workbench (GWB) version 11 Student Edition program. The activities of the elements dissolved in water were calculated with the GWB SpecE8 module. The model used to calculate the activity coefficient was Debye-Hückel because the ionic strengths were 0.020 and 0.026 mol/kg for the GHM and GRN hot springs, respectively. Based on the activity values obtained by the equilibrium model, the Act2 module of the GWB was used for the construction of the Porbouix diagrams considering the mineralogical species observed in each spring and the temperature, pH, and Eh conditions.

5 Results

5.1 Physicochemical characteristics of springs

The field parameters of the water samples for both sampling campaigns, as well as the concentrations of the major ions and some trace elements, are shown in Table 1.

The EC ranging between 1189–1382 µS/cm and TDS concentration 785–913 mg/L in the first field campaign of both hot springs are similar but lesser than the dry season [EC: 1940–1965 µS/cm; TDS: 1241–1258 mg/L (Fig. 3b)]. There is almost no change in pH in the hot springs for both campaigns, in the GHM hot spring is neutral and slightly more alkaline in the GRN hot spring (Fig. 3b). On the other hand, the sample of the GRN hot spring shows the temperature and SiO_2 concentration higher than those of the GHM hot spring in both seasons. The dominant ions in both springs are Na^+ and HCO_3^- (Fig. 3a, b); therefore, according to Giggenbach (1988), the thermal water of the study area was classified as peripheral. However, there is also an important concentration of Cl^- in the hottest spring (GRN) mainly in the dry season which tends to mature water (Fig. 3a) and, therefore Na-Cl type water. Arsenic is an element that has an important implication in geothermal systems. Since it is common for arsenic to be present in geothermal environments (Litter et al., 2019; López et al., 2012) it is important

Journal : Large 41513 | Article No : 173 | Pages : 20 | MS Code : 173 | Dispatch : 24-7-2021

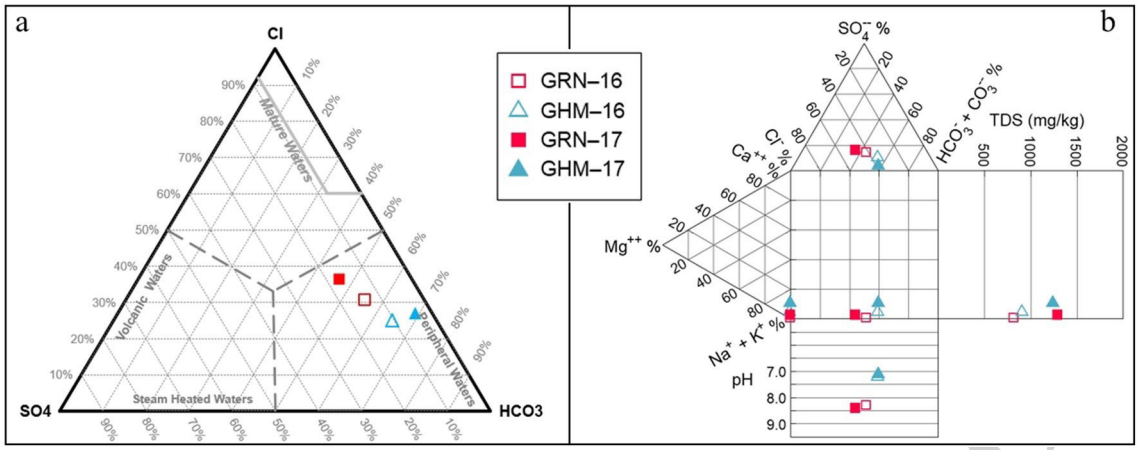

Fig. 3 Diagrams to classify thermal water; **a** water classification system proposed by Giggenbach (1988) using anions contents; **b** Durov Diagram obtained from the ionic concentrations in the GSS module of the Geochemist's Workbench (GWB) version 11 Student Edition program

to mention that the concentration of arsenic is high in both hot springs (300–650 µg/l).

5.2 Mineral composition in soil sediments

All the mineralogical identification of soil sediment samples collected near both hot springs and into the GRN hot spring by the different analytical techniques is shown in Table 2.

The most abundant mineral identified in both sites is plagioclase followed by quartz. Small barite crystals (< 1 mm) with tabular forms (Fig. 4a, b) and pyrite crystals (< 1 mm) were observed in both hot springs (Fig. 4c). A pyrite crystal with arsenic was identified using electron microprobe analysis, was found with soil sediments from the GHM hot spring (Fig. 4d). Unfortunately, it was not possible to distinguish between arsenopyrite and

Table 2 Compilation of all minerals observed and identified by the different techniques used in the study, as well as the semiquantitative proportion for XRD analyses

	Qualitative Observed by:			Semiquantitative XRD of soil sediments (wt %)		Semiquantitative XRD of sediments inside GRN hot spring (wt %)		Semiquantitative XRD fossil mud pool (wt %)
Mineralogical phases	Stereoscopic Microscopy	SWIR	ESEM and EPMA	Rancho Nuevo (GRN)	Los Mezquites (GHM)	Samples 1–3	Samples 4–6	Rancho Nuevo (GRN)
Plagioclase	**X**	N.A	N.A	**53%**	**64%**	**35–46%**	**35–39%**	N.O
Feldespar	**X**	N.A	N.A	N.O	N.O	**19–25%**	**17–25%**	**8%**
Quartz	**X**	N.A	N.A	**26%**	**28%**	**20–26%**	**19–33%**	N.O
Tridymite	N.O	N.A	N.A	N.O	N.O	**11–13%**	**7–9%**	N.O
Opal	N.O	**X**	N.A	N.O	N.O	N.O	N.O	**5%**
Calcite	N.O	N.O	N.A	**19%**	N.O	N.O	**8%**	N.O
Barite	**X**	N.O	**X**	N.O	**5%**	N.O	N.O	N.O
Pyrite	**X**	N.O	**X**	**< 5%**	**< 5%**	N.O	N.O	N.O
Stibnite	**X**	N.O	**X**	N.O	N.O	N.O	N.O	N.O
Montmorillonite	N.O	**X**	N.O	N.O	N.O	N.O	N.O	N.O
Smectite	N.O	N.O	N.O	**< 5%**	**< 5%**	**< 5%-6%**	**5–10%**	
Zeolite	N.O	N.O	N.O	N.O	N.O	N.O	**< 5%**	N.O
Kaolinite	N.O	**X**	N.O	N.O	N.O	N.O	N.O	**77%**
Alunite	N.O	N.O	N.O	N.O	N.O	N.O	N.O	**10%**

Cross mark (X) means that the mineralogical phase was observed

N.O. mineral not observed, *N.A.* mineral not analyzed

Journal : Large 41513 | Article No : 173 | Pages : 20 | MS Code : 173 | Dispatch : 24-7-2021

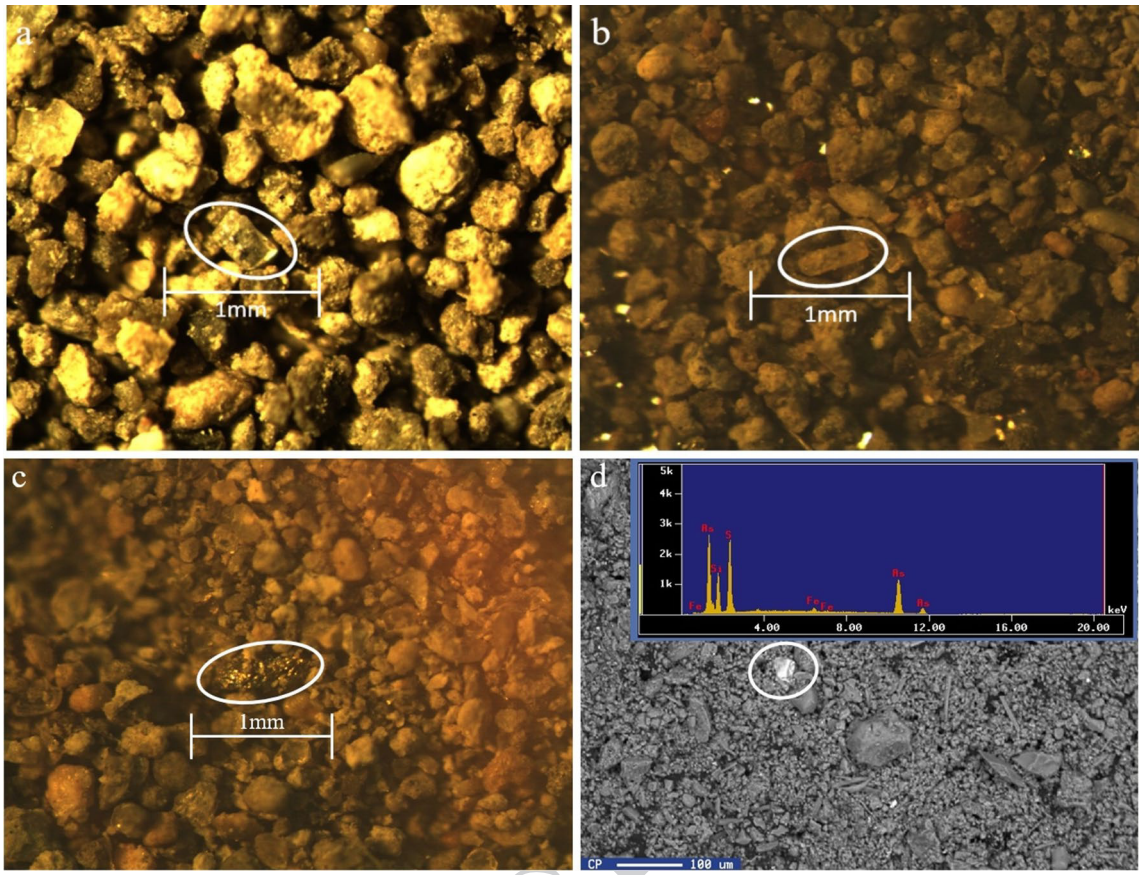

Fig. 4 Images of the sulfur minerals found at both hot springs. Barite crystals from the **a** GRN and **b** GHM hot springs identified by stereoscopic microscopy; **c** pyrite crystal identified by stereoscopic microscopy. **d** Pyrite with arsenic content crystal identified in the GHM hot spring by electron microprobe analysis. With circles highlight all minerals

As-bearing pyrite using XRD because of their deficient concentrations and very small size (< 50 µm), so it was not possible to separate.

Stibnite crystals were also identified in soil sediments of both hot springs by electron microprobe analysis. In general, stibnite has prismatic and columnar forms, which often have longitudinal striations or fractures characterized by smoothly curving surfaces. At the GRN hot spring, stibnite crystals were found in the fossil mud pool. These crystals are subangular and present tabular habits; however, they are very reworked and eroded, mainly at the corners, due to transport processes (Fig. 5a, b). On the other hand, at the GHM hot spring, the stibnite crystals are columnar, well-formed, and slightly eroded, thereby evidencing less transport than the GRN hot spring. The crystal shapes are tabular and cubic (Fig. 5c, d).

According to the SWIR analysis, other alteration minerals such as opal and montmorillonite are present in the soil sediment samples of both hot springs and kaolinite only in the GRN hot spring, specifically in the fossil mud pool (Fig. 6).

5.3 Mineral composition of fine grain fraction in soil sediments by XRD

The XRD analysis was used to identify with better accuracy all the mineralogical phases in fine grain fraction and to obtain a weight proportion (wt %) of each one (Table 2).

According to the XRD technique, the most abundant phase in wt % in both hot springs is plagioclase, followed by quartz and, with much less, pyrite. Barite was only identified in the GHM hot spring soil sediment in a low weight proportion (Fig. 7b, Table 2). Calcite was only found in the GRN hot spring, both on the soil sediment samples (Table 2) and in the sediment interacting with thermal water (Fig. 7a, Table 2); moreover, calcite was absent in the samples of the GHM hot spring, where the mineral was not identified.

After the clay grain fraction of the soil sediments were separated for XRD analysis by flocculation, poorly crystalline smectite was also identified in deficient weight proportion at both sampling sites (Table 2). That smectite shows no evidence of interstratification with other

Journal : Large 41513 | Article No : 173 | Pages : 20 | MS Code : 173 | Dispatch : 24-7-2021

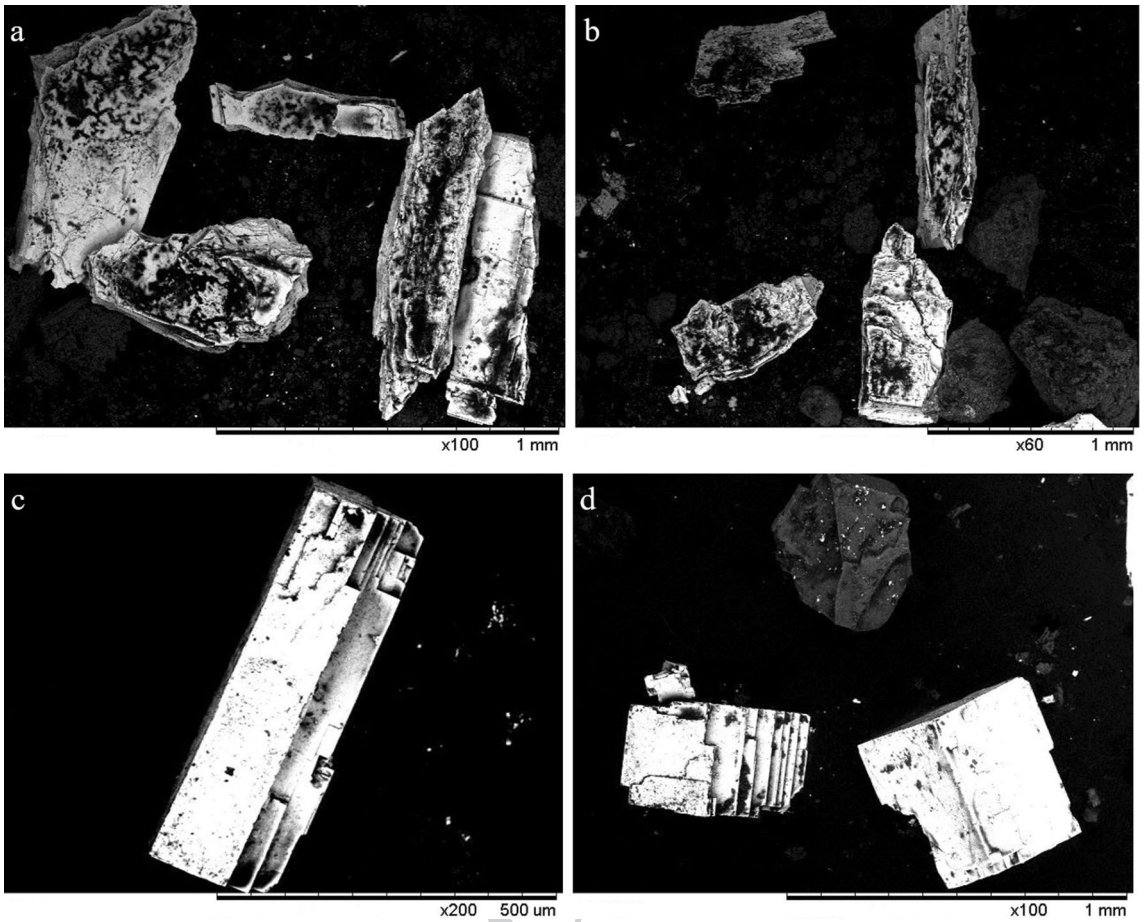

Fig. 5 Prismatic and columnar stibnite crystals identified by ESEM **a**, **b** from the fossil mud pool of the GRN hot spring sized between 0.5 and 1 mm and clearly eroded; **c**, **d** from soil sediments of the GHM hot spring sized 0.5 mm, then smaller and not eroded

minerals of the clay group. Other valuable alteration minerals identified by XRD in clay grain fraction, particularly in white crust formation of the fossil mud pool in the GRN hot spring (Fig. 2b, c) were alunite and kaolinite (Fig. 7c).

5.4 Hydrothermal alteration minerals in the GRN hot spring

The mineral associations identified inside the GRN hot spring through XRD analysis were: intermediate plagioclase with the highest weight proportion followed by quartz, potassium feldspar, and tridymite. Identification and detailed characterization of the clay minerals present are based on studies of clay-sized fractions by XRD, the presence of smectite in deficient weight proportion was recognized. Minerals from the zeolite group were also found in some samples. However, it was not possible to identify by XRD analyses due to the deficient weight proportion (Fig. 7d, Table 2). At the edge of the discharge zone of the GRN hot spring, crystallized calcite was present in the form of crusts (evidence with HCl 10%) in the field. Also, this was corroborated by the results of the XRD analysis, too (Table 2).

5.5 Sulfur isotopes

The two barite samples collected in the sediments show positive and similar isotope values and enrichment with both $\delta^{34}S_{barite}$ (‰ V-CDT) and $\delta^{18}O_{barite}$ (Table 3). The results for $\delta^{34}S_{barite}$ were 11.5‰ and 12.1‰ in the GRN hot spring and the GHM hot spring, respectively, and for $\delta^{18}O_{barite}$ were 7.9‰ and 7.6‰. These values, as shown in Fig. 8, evidence of the occurrence of mixing processes between Na-Cl water type with meteoric water in the geothermal system.

On the other hand, the $\delta^{34}S_{pyrite}$ the two pyrites of soil sediment samples showing ^{34}S-depleted values

Journal : Large 41513 | Article No : 173 | Pages : 20 | MS Code : 173 | Dispatch : 24-7-2021

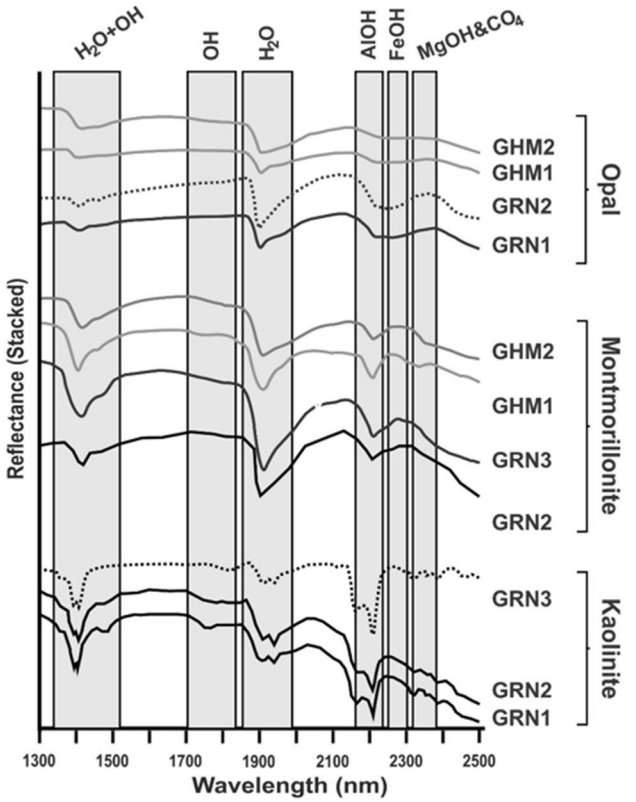

Fig. 6 SWIR spectra of soil sediments from the GRN and GHM hot springs. Opal, montmorillonite and kaolinite were identified

(Table 3), therefore negative values were found in both hot springs: − 9.7‰ in the GHM hot spring and − 15.2‰ in the GRN hot spring. The value of $\delta^{34}S$ of stibnite of the fossil mud pool is also depleted (− 9.9), however the $\delta^{34}S_{pyrite}$ of pyrite show different isotopic signature than the other samples having an enrichment whose value is + 1.5.

6 Discussion

6.1 Geology pattern of the geothermal system

The spatial distribution of both hot springs shows a N-S trend along with the Taxco-San Miguel de Allende fault system (Fig. 1). The thermal manifestations in San Bartolomé de Los Baños exhibits also N-S pattern, related to regional faulting of the San Miguel de Allende-Querétaro system (Aguirre-Díaz et al., 2005; Alaniz-Álvarez et al., 2001; Canet et al., 2019). Therefore, major geological structures and their spatial relationship, N-S Taxco-San Miguel de Allende fault system related to the intra-arc extension of the TMVB, control the occurrence of the GZRN, being an important geological feature in the region. Locally, the intersection of N-S regional trend and NW–SE and NE-SW faults controls the occurrence of thermal activity of the GRN and GHM hot springs. These structural patterns configure the southern limit of the El Bajío basin (Botero-Santa et al., 2015).

The intense volcanism and the high heat flow distinguish the central region of the TMVB (Pérez-López et al., 2011; Prol-Ledesma and Morán-Zenteno, 2019) being the most recent in the Pleistocene. It consisted of several andesitic lavas and monogenetic volcanoes related to the volcanic events of the last stage of the formation of the TMVB (Lesser y Asociados SA de CV 2000); it could suggest hypabyssal bodies in the area and promote a thermal source.

6.2 Hydrogeochemistry of hot spring waters

In dry season rise the EC and TDS of both springs, as well as ionic concentrations, mainly in the GRN hot spring, due to an evaporation process which causes a concentration of some ions in thermal water. EC and TDS of both springs in the dry season are higher than those of reporter for groundwater (150–1000 µS/cm and < 1000 mg/L respectively; Younger, 2007), indicating brackish water and influenced by thermal activity, mainly for the GRN hot spring.

The dominant ions in both springs are Na^+ and HCO_3^-; however, there is also an important concentration of Cl^- in the hottest spring (GRN) mainly in dry season indicating a dilution process in the thermal fluid caused by the rainy season and decreasing the chemical concentration of almost all ions. Concentrations of chloride are causing by a deep flow characterized by acidic and reducing conditions (Tóth, 2005). The high values of HCO_3^- may occur due to the dissolution and re-precipitation process of calcareous basement rock, as well as to a mixing process between that deep chloride water with shallow bicarbonate water. Also, although water from the springs is not for drinking, the concentrations of As and F^- are high according to Mexican regulations for the use and consumption of drinking water (NOM-127-SSA1).

6.3 Hydrothermal alteration

The analysis of the recent deposits (soil sediments) and their alteration minerals observed by different analytical techniques, as well as the mineralogy found from the white crust of the fossil mud pool evidence the occurrence and periodicity of hydrothermal activity in the study area.

According to SWIR and XRD results, non-crystalline silica phases (opal and tridymite) were identified in both springs of the GZRN, being opal a mineral often associated with hot springs. In the geothermal zone of San Bartolomé de los Baños, near to the GZRN, were also identified phases from the silica group as opal and quartz formed in permeable formations at shallow depths, below the steam

Journal : Large 41513 | Article No : 173 | Pages : 20 | MS Code : 173 | Dispatch : 24-7-2021

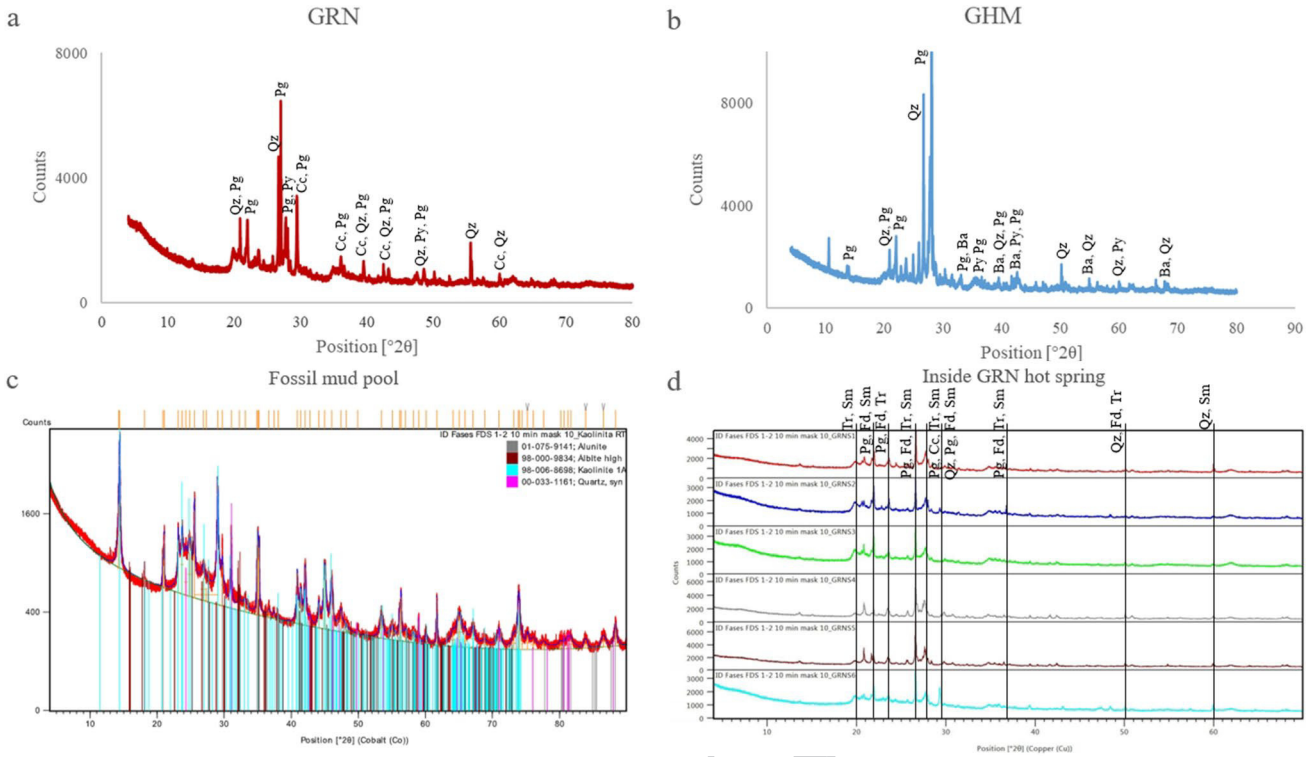

Fig. 7 Diffractograms of the fine grain fraction of soil sediment samples of the **a** GRN hot spring and **b** GHM hot spring. **c** Alunite and kaolinite identified from white crust formation of the fossil mud pool; **d** interior soil sediment samples of the GRN hot spring. Mineral abbreviations: *Ba* barite, *Cc* calcite, *Pg* plagioclase, *Py* pyrite, *Qz* quartz, *Cc* calcite, *Fd* feldspar, *Pg* plagioclase, *Qz* quartz, *Sm* smectite, *Tr* tridymite

Table 3 $\delta^{34}S$ values of barite, pyrite and stibnite samples in both hot springs and in the fossil mud pool

	$\delta^{34}S$ (‰ V-CDT)			$\delta^{18}O$ (‰)	
	GRN	GHM	Fossil mud pool GRN	GRN	GHM
Barite	+11.5	+12.1	–	+7.9	+7.6
Pyrite	− 9.7	− 15.2	+1.5	–	–
Stibnite	–	–	− 9.9	–	–

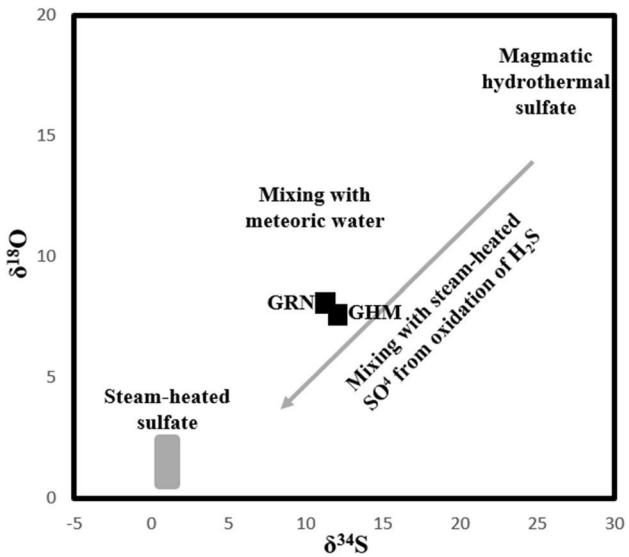

Fig. 8 Corroboration of the mixing process occurred in the GZRN according to the $\delta^{34}S$ (‰ V-CDT) and $\delta^{18}O_{barite}$ values in the GRN and GHM hot spring samples (original figure taken from Rye, 2005)

condensation zone (Canet et al., , 2015, 2019) and suggest temperatures of ~ 100 °C and moderate acidic conditions (Corbett & Leach, 1998). The presence of kaolinite in any environment indicates an advanced argillic alteration of volcanic rocks (Canet et al., 2015) and is considered, along the alunite, as a replacement of volcanic glass in the ignimbrites at shallow depths (Arellano et al. 1998), as it occurs in the Los Humeros geothermal field (Elders, et al., 2014) situated in the east of the TMVB. That advanced argillic alteration is also indicative of a low pH and is produced by H_2SO_4

Journal : Large 41513 | Article No : 173 | Pages : 20 | MS Code : 173 | Dispatch : 24-7-2021

formed by oxidation of H_2S at the surface (Elders et al., 2014) whose formation range of temperature is ~ 100 –to ~ 200 °C (Browne, 1978; Henley & Ellis, 1983; Reyes, 1990, 1992). Besides, kaolinite is associated with other minerals such as alunite, opal, tridymite (García-Valles et al., 2015) and all of them are also result of acidic conditions (Corbett & Leach, 1998).Therefore, kaolinite, alunite and opal found in the soil sediments of the GZRN are indicating an advanced argillic alteration in an acidic and oxidizing environment. The association of alunite and kaolinite suggests a relationship between the geothermal system and volcanic activity, as it happens in Acoculco and San Bartolomé de los Baños geothermal zones (Canet et al., 2015; Sánchez-Córdova et al., 2020 respectively) and is evidence of possible emission of partially acidic gases that occur in the past. Thus, the thermal conditions of the GZRN may have varied over time being is at first more acidic than now and/or altered minerals formed in acidic environment can have rapidly transported from deep to surface through the faults.

Other alteration minerals found in the GZRN, as well as in Los Humeros geothermal field, were quartz, calcite, pyrite and smectite are produced by neutral or alkaline fluids (Elders et al., 2014). Smectite, associated with opal and zeolites, was also found in the geothermal zone of San Bartolomé de los Baños and was defined as argillic alteration (Canet et al., 2019). However, in some cases the identification of smectite is ambiguous, owing to they can have their origin in hydrothermal or supergenic (weathering) processes (Thompson & Thompson, 1996), it is the case of the poorly crystalline smectite found in the GZRN. However, the smectite in the GZRN was identified along with other alteration minerals such as zeolite and calcite, then it is supposed to be formed by hydrothermal processes even though the XRD results does not show a clearly evidence of hydrothermal genesis of smectites. Zeolite is a mineral that changes as a function of temperature, rock, and fluid composition (Browne, 1978; Henley & Ellis, 1983; Reyes, 1990, 1992), then its precipitation in the GZRN is evidence of neutral to alkaline environment at a range of temperature of ~ 100 – ~ 200 °C.

Moreover, other siliceous phases were also identified in the GZRN, such as plagioclases, feldspars, and volcanic glass, as well as detrital components inherited from the igneous and pyroclastic rocks present in the stratigraphic column of the region. It is known that vitreous material in geothermal springs is usually altered, mainly to clay minerals, opal, zeolite, or calcite (web[1]), thus the thermal fluid interacted with the volcanic glass of Oligocene breached ignimbrites of the stratigraphic sequence in the study area could have been altered to those minerals because all of them were identified in the sediments of the hot springs.

6.4 Barite deposition and its connotation in the GZRN

Barite ($BaSO_4$) is a mineral mainly present in environments of hydrothermal origin (Canic et al., 2015; Dubé, 1988; Poole, 1988; Bloun, 1977; Strübel, 1967) especially in low-temperature fluids (< 120 °C) (Dubé, 1988; Hein et al., 2007; Mergner et al., 2012; Poole, 1988; Scheiber et al., 2012), Chemically, the precipitation of barite occurs due to its low solubility; the concentration of barium in water (Bodek et al., 1988) and its solubility increases when salinity increases at a temperature of 100 to 250 °C (Holland & Malinin, 1979). Barite can precipitate in some thermal springs under surface conditions through the alteration of volcanic rocks by acidic fluids or as a result of marine contribution as occurs in Mapachitos, Península de Baja California, another geothermal zone in northwestern of Mexico (Arellano-Ramírez et al., 2017; Rodríguez-Díaz et al., 2019). Accordingly, barite deposition may be interpreted as a near-surface assemblage (kaolinite + opal) produced under acidic and oxidizing conditions. Therefore, the barite precipitation in the soil sediments of the GZRN under surface conditions is suggested and it occurs due to the alteration of volcanic rocks by low temperature acidic fluids and oxidizing conditions as occurs also in the geothermal zone of San Bartolomé de los Baños. Besides, barite precipitation in both sites confirms the hydrothermal activity in the region.

The deep and acidic thermal fluid rises to the shallow aquifer where the conditions are oxidizing and colder causing a precipitation process of sulfates such as barite. This mineral suddenly precipitates as $BaSO_4$ at the subsurface due to the circulation of fluids driven by the high heat flow of the tectonic environment, as occurs in the southern California Continental Borderland, part of the broad San Andreas transform-fault plate boundary (Hein et al., 2007). In this system, tectonic and subsidence faults and fractures allow for the rapid ascension of thermal fluid.

Barium may associate with potassium in aqueous solutions and may even substitute potassium in rock-forming minerals containing this mineral (Naimy, 2008), and/or can be released from the plagioclases of the volcanic rock sequences during alteration reactions. These released ions are dissolved and incorporated into thermal fluid under oxidizing to semi-reducing, slightly acidic conditions in deep. Finally, the thermal fluid rises to the shallow aquifer causing cooling and a mixing process of late-stage hydrothermal fluids and meteoric water in a neutral and oxidizing environment, thus precipitating the barite (Rye, 2005). Therefore, these processes can occur for the formation and precipitation of barite in the GZRN. That mixing process is demonstrated in Fig. 8 where positive slope of the sulfur and oxygen–isotope data for barite is interpreted to represent mixing of

Journal : Large 41513 | Article No : 173 | Pages : 20 | MS Code : 173 | Dispatch : 24-7-2021

SO_4^{2-} derived from the disproportionation of magmatic SO_2 at depth (magmatic-hydrothermal) with sulfate formed during the oxidation of H_2S near the surface (Rye, 2005). Alternatively, barite in the environment may be a product of the interaction between thermal fluid and ignimbrites and andesites at depth given the affinity between barium and igneous rocks, particularly potassic and calc-alkaline volcanic rocks (Yavuz et al., 2002).

6.5 The implication of sulfide minerals and arsenic in the GZRN

Pyrite may precipitate when H_2S directly derived from igneous activity reacts with Fe-bearing wall rocks (Rye, 2005). Thus, it could have been a product of acidic alteration involving the oxidation of H_2S and precipitated from interaction and reaction processes between volcanic rocks and acidic fluids during the last volcanic activity in the region (between 1.3 to 0.83 Ma, CEAG, 2000). Moreover, few previous studies report the occurrence of stibnite, a sulfide mineral, in geothermal fields, yet some reports the presence of stibnite in low-sulfidation epithermal deposits (Lattanzi, 1999; McIver, 1997) and in the surface and subsurface zones of geothermal systems in Italy and El Salvador (Cappetti et al., 1995; Raymond et al., 2005), as is the case of the GZRN where stibnite was found at surface in soil sediments. It is known that antimony in geothermal systems is transported almost exclusively in liquid-phase geothermal fluids (Spycher & Reed, 1989). Its deposition is influenced by the decreasing temperature of hydrothermal fluids (~ 100- ~ 200 °C) and the change in pH conditions from acidic to neutral (Wilson et al., 2007). Besides, under nearly neutral pH (~ 7–8), stibnite and calcite can be deposited in thermal fluids (Kristmannsdottir 1989), comparable to what was observed in the GZRN.

On the other hand, arsenic is also commonly associated with pyrite (Webster & Nordstrom, 2003) and is indicative of some conditions and processes that occur in deep (Villanueva-Estrada et al., 2013). For instance, this metalloid can be leached along with other elements (such as antimony, barium, lithium and fluoride) and hydrogen sulfide (Ellis & Mahon, 1964; Maity et al., 2011; Webster & Nordstrom, 2003), their presence in thermal waters is evidence of Na-Cl water type in the reservoir, reducing conditions and high temperatures (Webster & Nordstrom, 2003). The assembly of these other elements with arsenic presents evidence of mixing processes in geothermal systems (Webster & Nordstrom, 2003). At temperatures of 150–250 °C, arsenic is usually found as As-bearing pyrite (Ballantyne & Moore, 1988; Bundschuh & Maity, 2015; Ewers & Keays, 1977) or can be released from andesites (Webster & Nordstrom, 2003).

Several studies in Guanajuato near to the study area similarly found also high concentrations of geogenic arsenic in groundwater wells with thermal activity (Landa Arreguín et al. 2021; Morales-Arredondo et al., , 2015, 2016; Rodríguez et al., 2006). It is related to the silicate weathering process in the region caused by water–rock interaction (Morales-Arredondo et al., 2020), then devitrification of volcanic glass and felsic rocks and finally the release of arsenic (Morales-Arredondo 2018). In the GZRN important concentrations of arsenic (Table 1) are also reported whose origin is related to: a) the weathering of volcanic rocks of the stratigraphic sequence in the study area of mostly acidic composition by the water–rock interaction; and/or, b) the leaching of As-bearing pyrite and finally its precipitation as As-bearing pyrite. The presence of arsenic in pyrite and its high concentrations of hot springs reveal reducing conditions and a range temperature of 150 to 250 °C in the reservoir, as well as confirm the mixing process occurred in the GZRN. The Na-Cl water type in the GRN hot spring sample of dry season reveals that the water flow is intermediate or even regional, then a high residence of thermal water.

6.6 Sulfur isotopes in the GZRN

The results for the sulfur isotopes in barite corroborate the mixing process (Fig. 8) between thermal fluid and meteoric water of shallow aquifer and show that an oxidation process occurs during the rise of thermal fluid because of the presence of atmospheric oxygen in subsurface zones, which produces an enrichment of ^{34}S relative to the starting material (Seal II 2006). It is due to the heavier isotope of sulfur is enriched in the higher oxidation state (Seal II et al. 2000). Considering the barites formed close and below the water table in Wiesbaden thermal spring system in Germany whose isotopic values of $\delta^{34}S$ are in a range from + 11.6‰ to + 14.7‰ and the fact that they are lesser positive than fossil barites located above the zone of the recently upwelling thermal water (+ 15‰ to + 16.9‰) (Wagner et al., 2005), the isotopes values of $\delta^{34}S$ of barites from the GRN (+ 11.5 ‰) and GHM (+ 12.1 ‰) hot springs may have formed recently and near to the water table.

Ohmoto and Lasaga (1982) have evaluated the kinetics of sulfur isotope exchange between SO_4^{2-} and H_2S and found that pH, temperature, and the total concentration of dissolved sulfur are dependent on the exchange rates. For instance, rates increase with increasing temperature and sulfur concentration and decreasing pH. So, it was found that for "typical" hydrothermal systems of near-neutral to slightly acidic conditions (pH 4 to 7), such as in the GZRN whose pH is acidic at depth and neutral to slightly alkaline on the surface and the isotopic equilibrium cannot reached temperatures below 200 °C. The positive value of $\delta^{34}S$ of pyrite in the fossil mud pool can be evidence of oxidizing processes of H_2S and SO_2 towards the surface.

Journal : Large 41513 | Article No : 173 | Pages : 20 | MS Code : 173 | Dispatch : 24-7-2021

6.7 Dissolution of the calcareous basement

Another process that appears to be occurring in the GZRN is the dissolution of the calcareous basement due to the possible slightly acidic composition of thermal fluid at depth. Despite carbonates having inverse solubility concerning temperature (Eq. 3), they can dissolve and precipitate in hydrothermal environments. For instance, any chemical reaction capable of releasing protons can produce carbonate dissolution (Eq. 1), including the oxidation reaction of H_2S to sulfate (Eq. 2) (Corbella et al., 2007), which is detailed at following:

$$CaCO_{3(s)} + 2H^{+} = Ca^{2+} + CO_{2(aq)} + H_2O \quad (1)$$

$$H_2S_{(aq)} + 2O_{2(aq)} = SO_4^{2-} + 2H^{+} \quad (2)$$

The acidity of the protons (H^+) associating with dissolved carbonate ions (CO_3^{2-}) in the thermal fluid leads to the formation of bicarbonates (HCO_3^-), thereby increasing the pH (> 6.3) (Appelo & Postma, 2005). Also, according to Nicholson (1993), water contained in limestone or water interacting with rocks rich in carbonates will have a high concentration of bicarbonates. These processes, as well as mixing process with shallow water, may cause high concentrations of bicarbonate in both hot springs, whose chemical composition indicated that HCO_3^- was the dominant anion.

Notably, the solubility of calcite is retrograde and is expressed by a reaction defined as dissolution–precipitation (Nicholson, 1993), as follows:

$$Ca^{2+}_{(aq)} + 2HCO^{-}_{3(aq)} = CaCO_{3(s)} + H_2O_{(l)} + CO_{2(g)} \quad (3)$$

Applying the Le Chatelier principle in Eq. (3), an increase in CO_2 produces $CaCO_3$ dissolution, and a decrease in CO_2 produces $CaCO_3$ precipitation (Appelo & Postma, 2005). Calcite appears to be forming in the discharge zones of the GZRN because the ascension of thermal fluid to the surface produces a loss of CO_2. The dissolution of the calcareous basement produces high contents of calcium in thermal water. However, the Ca^{2+} can be precipitate as calcic plagioclase, mineral with a greater presence in the area.

The thermal fluid is being saturated with calcite as a result of the dissolution of basement rocks, it ascends through faults and is modified by boiling and mixing processes, leading to an increase in pH and pressure and a decrease in temperature. Finally, the thermal water arrives at the surface, and calcite is precipitated in the discharge zone of the springs.

6.8 Final remarks on mineral deposition in the GZRN

Phase diagrams were made to confirm the presence of some alteration minerals observed and identified by the different

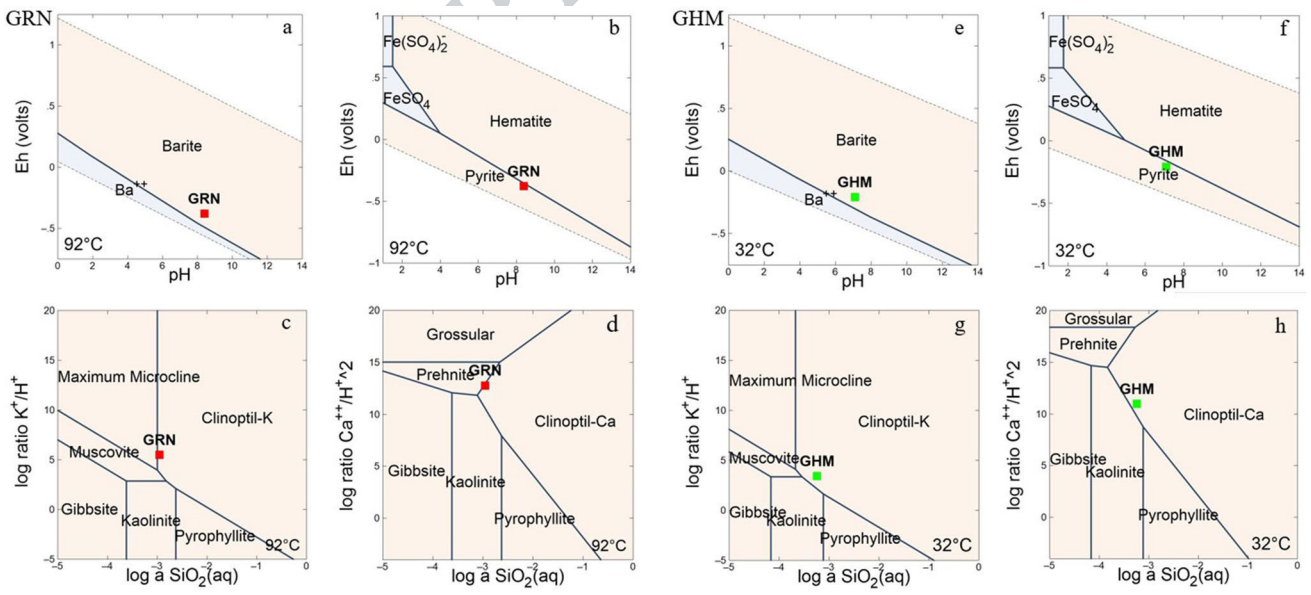

Fig. 9 Stability and activity diagrams of the GRN and GHM hot spring samples: stability diagram of **a** barite and **b** pyrite in the GRN hot spring samples. Activity diagrams: **c** clinoptilolite K and **d** clinoptilolite Ca in the GRN hot spring samples. Stability diagrams showing the precipitation of **e** barite and **f** pyrite in the GHM hot spring samples. Activity diagrams showing the precipitation of **g** clinoptilolite K and **h** clinoptilolite Ca in the GHM hot spring samples

Journal : Large 41513 | Article No : 173 | Pages : 20 | MS Code : 173 | Dispatch : 24-7-2021

analytical techniques (microscopy, electron microprobe, and XRD) used in the geological study. The diagrams of both springs were made considering their specific conditions. According to the Eh–pH stability diagrams, barite (Fig. 9a and 9e) and pyrite (Fig. 9b and 9f) can precipitate in both springs. Moreover, the activity diagrams demonstrate that zeolites can also be formed, which, owing to the stability diagrams, are defined as calcium and potassium clinoptilolites ($(Ca,K)_6(Si_{30}Al_6)O_{72}$*$20H_2O$) (Fig. 9c, d, g, h).

Meteoric water is infiltrated through faults; subsequently heated at depth by a convective process and/or by a magmatic source whose depth is unknown. The acidic environment in the reservoir zone can be caused by emission of partially acid gases of that magmatic source or by partially acidic gases released of the last volcanic activity in the region producing the dissolution of the calcareous basement rock. During the rise of the thermal fluid (Na-Cl water type) through the up-flow zone, the H_2S suffers an oxidation process, the formation of H_2SO_4, and the precipitation of kaolinite, alunite, pyrite, and opal in an acidic environment. Under similar acidic and oxidizing conditions but at lower temperatures, the barite precipitates in subsurface zones. Finally, the thermal fluid reaches the shallow aquifer (Na-HCO_3^- type water), thus the mixing process is carried out, therefore the conditions of the geothermal system are also modified from acidic to neutral-slightly alkaline, decreasing the temperature of the thermal fluid and precipitating alteration minerals such as calcite, stibnite, zeolite and smectite near to the surface or even in the discharge zone.

7 Conclusions

In the GZRN the alteration minerals and the geothermal activity are influenced by the Taxco-San Miguel de Allende regional fault, besides of the recent volcanism of the Llano Grande and La Gavia volcanoes in the study area, therefore the GZRN is defined as a convective geothermal system controlled by fault systems of an extensional tectonic regime with probable magmatic contribution (Fig. 10).

According to some altered minerals identified, such as kaolinite, alunite, opal, pyrite, stibnite, zeolite, as well as the high concentrations of arsenic found in both hot springs and its association with pyrite in soil sediments, the reservoir temperature range in the GZRN is ~ 150 to ~ 200 °C, corresponding to an intermediate-temperature system, however it is recommended to corroborate with geothermometers and mineral saturation indexes.

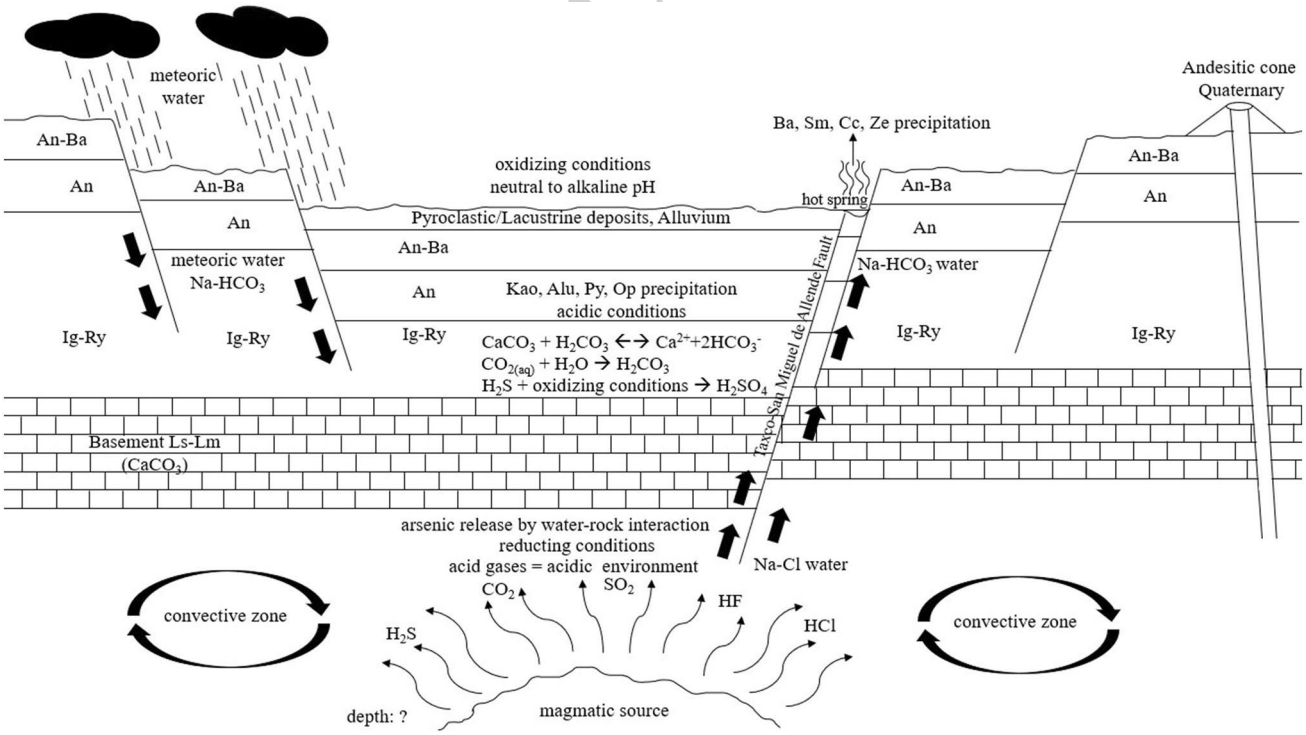

Fig. 10 Conceptual model of the GZRN according to the alteration minerals identified in the study area. Abbreviations: *An* andesite, *Ba* basalt, *Ig* ignimbrite, *Ry* rhyolite, *Ls* limestone, *Lm* limonite, *Ba* barite, *Sm* smectite, *Cc* calcite, *Ze* zeolite, *Op* opal, *Kao* kaolinite, *Alu* alunite, *Py* pyrite

Journal : Large 41513 | Article No : 173 | Pages : 20 | MS Code : 173 | Dispatch : 24-7-2021

The degree of development of each mineral assemblage varies from site to site in the GZRN area, resulting in the formation of inactive (for instance, hydrothermal activity decreases in the GHM hot spring) or active hot springs that reflect the long-lived evolution and high residence of hydrothermal fluids, so it is assumed that thermal activity in the region has been intermittent and varied over time being at first more acidic than now.

The presence of kaolinite and alunite reveal an advanced argillic alteration of different volcanic rocks of the study area and are considered as a replacement of volcanic glass of the Oligocene breached ignimbrites, and along with opal, pyrite and barite reveal an acidic and oxidizing environment. However, barite is formed recently at low temperatures and near to the water table. The precipitation of calcite and stibnite at the surface is influenced by the decreasing temperature of hydrothermal fluid due to the mixing process with a shallow aquifer (meteoric water) and the change in pH conditions from acidic to neutral (~7–8), therefore these minerals are evidence of change conditions in the geothermal system. Zeolite and smectite deposition occur by low-temperature thermal fluid in a neutral or alkaline environment. On the other hand, the presence of arsenic, along with high concentrations of fluorides, corroborate the mixing process in the GZRN and reveals high residence of thermal fluid under reducing conditions and high temperatures, as well as an intermediate or even regional flow water and whose evidence is the Na-Cl type pf water of the GRN hot spring.

The most important process that is occurring in the GZRN is the water–rock interaction between geothermal fluid and rocks of the stratigraphic sequence of the region including the basement rock, causing the formation of alteration minerals; some of them are in thermodynamic equilibrium.

Acknowledgements Funding was provided by the Mexican Center for Innovation in Geothermal Energy (Centro Mexicano de Innovación en Energía Geotérmica [CeMIE-Geo]): CONACyT-SENER-Energetic Sustainability Sectorial Fund (Fondo Sectorial CONACyT-SENER-Sustentabilidad Energética), grant number 207032-2013-04, "Map of geothermal provinces based on fluid geochemistry and aquifer distribution: A tool for the exploration and development of conventional geothermal resources" (*Mapa de provincias geotérmicas a partir de la geoquímica de fluidos y la distribución de acuíferos: herramienta para la exploración y desarrollo de los recursos geotérmicos convencionales*). The authors express their gratitude to Teresa Pi Puig (Geology Institute, UNAM) for her support in the XRD analyses and Carlos Linares López (Geophysics Institute, UNAM) for his assistance with the use of the EPMA equipment. We also thank Blanca Xóchitl Felipe Martínez for performing the ionic chromatography measurements, Ofelia Morton-Bermea and Elizabet Hernández-Álvarez for carrying out the trace element analysis by ICP-MS. The authors thank Consuelo Macías Romo for conducting the mineral separation experiments (Mineral Separation Laboratory II, Geology Institute, UNAM) and Juan Tomás Vázquez (Geosciences Institute, UNAM-Juriquilla) for making the thin sections.

References

4500-S2-SULFIDE. (2017). *Standard methods for the examination of water and wastewater*. https://doi.org/10.2105/SMWW.2882.096

4500-SiO_2 SILICA. (2017). *Standard methods for the examination of water and wastewater*. https://doi.org/10.2105/SMWW.2882.095

Aguirre-Díaz, G. J., & López-Martínez, M. (2001). The Amazcala caldera, Queretaro, Mexico: Geology and geochronology. *Journal of Volcanology and Geothermal Research, 111*, 203–218.

Aguirre-Díaz, G. J., & López-Martínez, M. (2003). *La caldera de Apaseo, Guanajuato, Geología y geocronología de una nueva caldera en el sector central del Cinturón Volcánico Mexicano* (p. 308). GEOS.

Aguirre-Díaz, G. J., Nieto-Obregón, J., & Zúñiga, F. R. (2005). Seismogenic basin and range intra-arc normal faulting in the central Mexican Volcanic Belt, Querétaro, México. *Geological Journal, 40*, 215–243.

Alaniz-Álvarez, S. A., & Nieto-Samaniego, A. F. (2005). El sistema de fallas Taxco-San Miguel de Allende y la Faja Volcánica Transmexicana, dos fronteras tectónicas del centro de México activas durante el Cenozoico. *Boletín de la Sociedad Geológica Mexicana, Volumen Conmemorativo del Centenario Grandes Frontertas Tectónicas de México, LVII*(I), 65–82.

Alaniz-Álvarez, S. A., & Nieto-Samaniego, A. F. (2007). The Taxco-San Miguel de Allende fault system and the Trans-Mexican Volcanic Belt: Two tectonic boundaries in central Mexico active during the Cenozoic. *Geology of Mexico: Celebrating the Centenary of the Geological Society of Mexico, USA* (pp. 301–316). The Geological Society of America.

Alaniz-Álvarez, S. A., Nieto-Samaniego, A. F., Reyes-Zaragoza, M. A., Orozco-Esquivel, M. T., Ojeda-García, A. C., & Vasallo-Morales, L. F. (2001). Estratigrafía y deformación de la región de San Miguel de Allende-Querétaro. *Revista Mexicana de Ciencias Geológicas, 18*, 129–148.

Appelo, C. A. J., & Postma, D. (2005). *Geochemistry, groundwater and pollution* (2nd ed.). Rotterdam.

Arce, J. L., Macías, J. L., Rangel, E., & Layer, P. (2012). Late Pleistocene rhyolitic explosive volcanism at Los Azufres Volcanic Field, central Mexico. In J. Aranda-Gómez, & G. Tolson (Eds.), Field Guide 25, GSA Cordilleran Section Meeting.

Arellano-Ramírez, Y., Kretzschmar, T. G., & Hernández-Martínez, R. (2017). Water-rock microbial interactions in the hydrothermal spring of Puertecitos, Baja California, Mexico. *Procedia Earth and Planetary Science, 17*, 865–868.

Ármansson, H. (2009). Application of geochemical methods in geothermal exploration. Short Course IV on exploration for geothermal resources, organized by UNU-GTP, KenGen and GDC, at Lake Naivasha, Kenya.

Arredondo, B. (2012). *Los antiguos baños de San Bartolomé Aguas Calientes. Apaseo el Alto, Guanajuato*. Retrieved November 6, 2019, from http://vamonosalbable.blogspot.com/2012/03/los-antiguos-banos-de-sanbartolome.html.

Ballantyne, J. M., & Moore, J. N. (1988). Arsenic geochemistry in geothermal systems. *Geochimica et Cosmochimica Acta, 52*, 475–483.

Blount, C. W. (1977). Barite solubilities and thermodynamic quantities up to 300 °C and 1400 bars. *American Mineralogist, 62*, 942–957.

Bodek, I., Lyman, W. J., Reehl, W. F., & Rosenblatt, D. H. (Eds.). (1988). *Environmental inorganic chemistry: Properties, processes, and estimation methods*. Pergamon Press.

Bolós, X., Cifuentes, G., Macías, J. L., Sosa-Ceballos, G., García-Tenorio, F., & Albor, M. (2019). Geophysical imaging of fluid circulation and its relation with the structural system of Cerritos Colorados geothermal field, La Primavera caldera

(Mexico). *Journal of Volcanology and Geothermal Research, 369*, 238–249.

Botero-Santa, P. A., Alaniz-Álvarez, S. A., Nieto-Samaniego, A. F., López-Martínez, M., Levresse, G., Xu, S., & Ortega-Obregón, C. (2015). Origen y desarrollo de la cuenca El Bajío en el sector central de la Faja Volcánica Transmexicana. *Revista Mexicana de Ciencias Geológicas, 32*(1), 84–98.

Browne, P. R. L. (1970). Hydrothermal alteration as an aid in investigating geothermal fields. *Geothermics, 2*, 564–570.

Browne, P. R. L. (1978). Hydrothermal alteration in active geothermal fields. *Annual Reviews of Earth and Planetary Science, 6*, 229–250.

Bundschuh, J., & Maity, J. P. (2015). Geothermal arsenic: Occurrence, mobility and environmental implications. *Renewable Sustainable Energy Reviews, 42*, 1214–1222.

Campos-Enríquez, J., & Sánchez-Zamora, O. (2000). Crustal structure across southern Mexico inferred from gravity data. *Journal of South American Earth Sciences, 13*(6), 479–489.

Canet, C., Hernández-Cruz, B., Jiménez-Franco, A., Pi, T., Peláez, B., Villanueva-Estrada, R. E., Alfonso, P., González-Partida, E., & Salinas, S. (2015). Combining ammonium mapping and short-wave infrared (SWIR) reflectance spectroscopy to constrain a model of hydrothermal alteration for the Acoculco geothermal zone, Eastern Mexico. *Geothermics, 53*, 154–165.

Canet, C., Rodríguez-Díaz, A., Bernal, I. D., Pi, T., Sánchez-Córdova, M. M., Núñez-Useche, F., Villanueva-Estrada, R., Molina, G., Reich, M., Peláez, B., Jiménez-Salgado, E., González-Partida, E., Sandoval-Medina, F., & Carrillo-Sánchez, C. B. (2019). Consideraciones sobre el sistema geotérmico de San Bartolomé de los Baños, Guanajuato (México), desde un análisis de la alteración hidrotermal y las inclusiones fluidas. *Geofísica Internacional, 58*(3), 229–246.

Canic, T., Baur, S., Bergfeldt, T., & Kuhn, D. (2015). Influences on the Barite Precipitation from Geothermal Brines. World Geothermal Congress, Melbourne, Australia, 19–25 April.

Cappetti, G., D'Olimpio, P., Sabatelli, F., & Tarquini, B. (1995). Inhibition of antimony sulphide scale by chemical additives: laboratory and field test results. In *Proceedings of the 1995 World Geothermal Congress, Florence, Italy* (pp. 2503–2507). May 18–31, 1995.

Carrasco-Núñez, G., López-Martínez, M., Hernández, J., & Vargas, V. (2017). Subsurface stratigraphy and its correlation with the surficial geology at Los Humeros geothermal field, eastern Trans-Mexican Volcanic Belt. *Geothermics, 67*, 1–17.

CEAG. (2000). Actualización del balance subterráneo de los acuíferos de Guanajuato. Comisión Estatal del Agua de Guanajuato, Guanajuato, Gto. Reporte Interno (p. 87).

Cerca-Martínez, L. M., Aguirre-Díaz, G. J., & López-Martínez, M. (2000). The geologic evolution of the southern Sierra de Guanajuato, Mexico: A documented example of the transition from the Sierra Madre Occidental to the Mexican Volcanic Belt. *International Geology Review, 42*, 131–151.

Clark, R. N., Swayze, G. A., Wise, R. A., Livo, K. E., Hoefen, T. M., Kokaly, R. F., & Sutley, S. J. (2007). *USGS Digital Spectral Library splib06a, USGS Digital Data Series, 231*. Retrieved May 17, 2020, from http://speclab.cr.usgs.gov.

Corbella, M., Cardellach, E., & Ayora, C. (2007). Disolución y precipitación de carbonatos en sistemas hidrotermales. Implicaciones en la génesis de depósito tipo MVT. *Boletín de la Sociedad Geológica Mexicana, LIX*(1), 83–99.

Corbett, G. J., & Leach, T. M. (1998). Southwest Pacific rim gold–copper systems; structure, alteration and mineralization. *Society of Economic Geologists, Special Publications Series, 6*, 238.

Demant, A. (1978). Características del eje neovolcánico transmexicano y sus problemas de interpretación. *Universidad Nacional Autónoma de México, Instituto de Geología, Revista, 2*, 172–187.

Dubé, T. E. (1988). Tectonic significance of Upper Devonian igneous rocks and bedded barite, Roberts Mountains allochthon, Nevada, U.S.A. In *Devonian of the world; Proceedings of the Second International Symposium on the Devonian System, Volume II, Sedimentation: Canadian Society of Petroleum and Geologists Memoir* (Vol. 14, pp. 235–249).

Elders, W. A., Izquierdo-Montalvo, G., Aragón-Aguilar, A., Tovar-Aguado, R., & Flores-Armenta, M. (2014). Significance of deep zones of intense bleaching and silicification in the Los Humeros high-temperature geothermal field, México: Evidence of the effects of acid alteration. *Geothermal Resources Council Transact, 38*, 497–502.

Ellis, A. J., & Mahon, W. A. J. (1964). Natural hydrothermal system and experimental hot-water/rock interactions. *Geochimica et Cosmochimica Acta, 28*, 1323–1357.

Ewers, G. R., & Keays, R. R. (1977). Volatile and precious metal zoning in the Broadlands geothermal field, New Zealand. *Economic Geology, 72*, 1337–1354.

Ferrari, L., Orozco-Esquivel, T., Manea, V., & Manea, M. (2012). The dynamic history of the Trans-Mexican Volcanic Belt and the Mexico subduction zone. *Tectonophysics, 522*, 122–149.

García-Valles, M., Pi, T., Alfonso, P., Canet, C., Martínez, S., Jiménez-Franco, A., Tarrago, M., & Hernández-Cruz, B. (2015). Kaolin from Acoculco (Puebla, Mexico), as raw material: Mineralogical and thermal characterization. *Clay Minerals, 50*, 405–416.

Garduño-Monroy, V. H., Spinnler, J., & Ceragioli, E. (1993). Geological and structural study of the Chapala Rift, state of Jalisco, Mexico. *Geofísica Internacional, 32*(3), 486–499.

Giesemann, A., Jäger, H. J., Norman, A. L., Krouse, H. R., & Brand, W. A. (1994). Online sulfur-isotope determination using an elemental analyzer coupled to a mass spectrometer. *Analytical Chemistry, 66*(18), 2816–2819.

Giggenbach, W. F. (1988). Geothermal solute equilibria. Derivation of Na-K-Ca-Mg geoindicators. *Geochimica et Cosmochimica Acta, 52*, 2749–2765.

Gómez-Tuena, A., Orozco-Esquivel, M. T., & Ferrari, L. (2005). Petrogénesis ígnea de la Faja Volcánica Trans-Mexicana. Boletín de la Sociedad Geológica Mexicana. *Volumen Conmemorativo Del Centenario LVII, 3*, 227–283.

Gómez-Tuena, A., Orozco-Esquivel, M. T., & Ferrari, L. (2007). Igneous petrogenesis of the Trans-Mexican Volcanic Belt. *Geology of Mexico: Celebrating the Centenary of the Geological Society of Mexico* (pp. 129–181). The Geological Society of America.

Gutiérrez-Negrín, L. C. (2015). Mexican geothermal plays. In *Proceedings of the World Geothermal Congress* (p. 9).

Hein, J. R., Zierenberg, R. A., Maynard, J. B., & Hannington, M. D. (2007). Barite-forming environments along rifted continental margin, Southern California Borderland. *Dee-Sea Research II, 54*, 1327–1349.

Henley, R. W., Ellis, A. J. (1983). *Geothermal systems ancient and modern: A geochemical review. Earth-science reviews* (Vol. 19, pp. 3–15). Elsevier.

Hillier, S. (2000). Accurate quantitative analysis of clay and other minerals in sandstones by XRD: Comparison of a Rietveld and a reference intensity ratio (RIR) method and the importance of sample preparation. *Clay Minerals, 35*(1), 291–302.

Holland, H. D., & Malinin, S. D. (1979). Oxygen and hydrogen isotope relationship in hydrothermal mineral deposits. In H. L. Barnes (Ed.), *Geochemistry of hydrothermal ore deposits* (2nd ed., pp. 461–508). Wiley.

Juárez-Arriaga, E., Böhnel, H., Carrasco-Nuñez, G., & Nasser Mahgoub, A. (2018). Paleomagnetism of Holocene lava flows from Los Humeros caldera, eastern Mexico: Discrimination of

volcanic eruptions and their age dating. *Journal of South American Earth Sciences, 88*, 736–748.

Kristmannsdóttir, H. (1989). Types of scaling occurring by geothermal utilization in Iceland. *Geothermics, 18*, 183–190.

Landa-Arreguín, J. F. A., Villanueva-Estrada, R. E., Ortega-Gutiérrez, J. E., Morales-Arredondo, J. I., Amézaga-Campos, B. S., & Armienta-Hernández, M. A. (2021). Presence of geogenic arsenic caused by thermal activity in the Celaya Valley Aquifer: Environmental implications. In *The 8th International Congress and Exhibition on Arsenic in the Environment, Wageningen, Netherlands*, 7th to 9th June.

Landa-Arreguín, J. F. A., Villanueva-Estrada, R. E., Rocha-Miller, R. G., Rodríguez-Salazar, M. T. J., Rodríguez-Díaz, A. A., & Hernández-Mendiola, E. (2017). *Resultados preliminares del estudio geoquímico de la zona geotérmica de Rancho Nuevo, Guanajuato*. Memorias del XXIV Congreso Anual de la Asociación Geotérmica Mexicana, Morelia, Mich., 29–31 marzo.

Lattanzi, P. (1999). Epithermal precious metal deposits of Italy—An overview. *Mineralium Deposita, 34*, 630–638.

Lesser y Asosiados, S. A. de C.V. (2000). *Seguimiento del estudio hidrogeológico y modelo matemático del acuífero del Valle de Celaya, Gto*. Seguimiento.

Litter, M. I., Armienta, M. A., Villanueva-Estrada, R. E., Villaamil Lepori, E., & Olmos, V. (2019). Arsenic in Latin America. *Science Reviews—From the End of the World, 1*, 54–73.

López, D. L., Bundschuh, J., Birkle, P., Armienta, M. A., Cumbal, L., Sracek, O., Cornejo, L., & Ormachea, M. (2012). Arsenic in volcanic geothermal fluids of Latin America. *Science of Total Environment, 429*, 57–75.

Lynne, B. Y., & Campbell, K. A. (2004). Morphologic and minerlogic transitions from opal-A to opal-CT in low-temperature siliceous sinter diagenesis, Taupo Volcanic Zone, New Zealand. *Journal of Sedimentary Research, 74*, 561–579.

Maity, J. P., Liu, C. C., Nath, B., Bundschuh, J., Kar, S., Jean, J. S., Bhattacharya, P., Liu, J. H., Atla, S. B., & Chen, C. Y. (2011). Biogeochemical characteristics of Kuan-Tzu-Ling, Chung-Lun and Bao-Lai hot springs in southern Taiwan. *Journal Environmental Science and Health, Part A, 46*, 1207–1217.

McIver, D. A. (1997). Epithermal precious metal deposits: Physicochemical constraints, classification characteristics, and exploration guidelines. Retrieved May 28, 2020, from https://core.ac.uk/download/pdf/11985289.pdf.

Mergner, H., Eggeling, L., Kölbel, T., Münch, W., & Genter, A. (2012). *Geothermische Stromerzeugung: Bruchsal und Soultz-sous-Forêts, Mining Geology* (pp. 666–673).

Moeck, I. S. (2014). Catalog of geothermal play types based on geologic controls. *Renewable Sustainable Energy Review, 37*, 867–882.

Molina-Martínez, A. (2013). Case history of los Azufres—Conceptual modelling in a Mexican geothermal field. Presented at *Short course V on Conceptual Modelling of Geothermal Systems*, Santa Tecla, El Salvador, February 24–March 2.

Moore, D. M., & Reynolds, R. C., Jr. (1997). *X-ray diffraction and the identification and analysis of clay minerals* (p. 378). Oxford University Press.

Morales-Arredondo, I., Armienta Hernández, M. A., Ortega-Gutiérrez, J. E., Flores-Ocampo, I. Z., & Flores-Vargas, R. (2020). Evaluation of the carbon dioxide behavior in a thermal aquifer located at Central Mexico and its relation to silicate weathering. *International Journal Earth Science and Technology*

Morales-Arredondo, I., Rodríguez, R., Armienta, M. A., & Villanueva-Estrada, R. E. (2016). The origin of groundwater arsenic and fluorine in a volcanic sedimentary basin in central Mexico: A hydrochemistry hypothesis. *Hydrogeology Journal, 25*(1), 1–16.

Morales-Arredondo, I., Villanueva-Estrada, R. E., Rodríguez, R., & Armienta, M. A. (2015). Geological, hydrogeological and geothermal factors associated to the origin of arsenic, fluoride, and groundwater temperature in a volcanic environment "El Bajío Guanajuatense" Mexico. *Environmental Earth Sciences, 74*, 5403–5415.

Morales-Arredondo, J. I., Armienta-Hernández, M. A., Hernández-Mendiola, E., Estrada-Hernández, R. E., & Morton-Bermea, O. (2018). Hydrogeochemical behavior of uranium and thorium in rock and groundwater samples from southeastern of El Bajío Guanajuatese, Guanajuato. *Mexico. Environmental Earth Sciences., 77*, 567.

Naimy, G. (2008). *Aquatic geochemistry of barium in basaltic terrain.* Iceland, Sigillum Universitatis Islandiae, Thesis.

Nicholson, K. (1993). *Geothermal fluids* (p. 263). Springer Nature.

Nieto-Samaniego, A. F., Alaniz-Alvarez, S. A., Cerca-Martínez, M. (1999). Carta Geológico-Minera San Miguel de Allende, F14C54, San Miguel de Allende, escala 1:50000. Aguascalientes, Ags., México, Consejo de Recursos Minerales, un mapa, secciones y texto explicativo.

NOM-014-SSA1-1993. *Procedimientos sanitarios para el muestreo de agua para uso y consumo humano en sistemas de abastecimiento de agua públicos y privados. Estados Unidos Mexicanos-Secretaria de Salud*. Noviembre, 1993 NOM 127

NOM-127-SSA1-1994. *Norma Oficial Mexicana Salud ambiental, agua para uso y consumo humano-límites permisibles de calidad y tratamientos a que debe someterse el aguapara su potabilizacion* (MODIFICADA 2000).

Ohmoto, H., & Lasaga, A. C. (1982). Kinetics of reactions between aqueous sulfates and sulfides in hydrothermal systems. *Geochimica Et Cosmochimica Acta, 46*, 1727–1745.

Ortega-Gutiérrez, J. E., (2019). *Caracterización hidrogeoquímica del agua subterránea en el municipio de Villagrán, Gto: procesos relacionados con la presencia de arsénico y fluoruro en el acuífero*. Escuela Superior de Ingeniería y Arquitectura, Instituto Politécnico Nacional (IPN). Thesis.

Pérez-López, R., Legrand, D., Garduño-Monroy, V. H., Rodríguez-Pascua, M. A., & Giner-Robles, J. L. (2011). Scaling laws of the size-distribution of monogenetic volcanoes within the Michoacán-Guanajuato Volcanic Field (Mexico). *Journal of Volcanology Geothermal Research, 201*(1–4), 65–72.

Pérez-Martínez, I., Villanueva-Estrada, R. E., Cardona-Benavides, A., Rodríguez-Díaz, A. A., Rodríguez-Salazar, M. T., & Guadalupe, J. (2020). Hydrogeochemical reconnaissance of the Atotonilco el Alto-Santa Rita geothermal system in the northeastern Chapala graben in Mexico. *Geothermics, 83*, 101733.

Pita-de la Paz, C., Sánchez-Galindo, A., Garfias-Quezada, J. A., García-García, E., Villanueva-Estrada, R. E., Rocha-Miller, R., Bernard-Romero, R., Rodríguez-Díaz, A. A., Rubio-Ramos, M. A., & Salazar-Medina, E. (2016). Integración de metodologías geofísicas, geoquímicas y geológicas para la evaluación geotérmica de la localidad Rancho Nuevo, Celaya, Guanajuato, México. Reunión Anual de la UGM, v36, 1 noviembre, p. 173.

Poole, F. G. (1988). Stratiform barite in Paleozoic rocks of the Western United States. In Stuttgart, E. (Ed.) *Proceedings of the Seventh Quadrennial IAGOD Symposium* (pp. 309–319). Schweizerbartsche Verlangsbuchhandlung.

Prol-Ledesma, R. M., Carrillo-de la Cruz, J. L., Torres-Vera, M. A., Membrillo-Abad, A. S., & Espinoza-Ojeda, O. M. (2018). Heat flow map and geothermal resources in Mexico. *Terra Digitalis, 2*(2), 1–38.

Prol-Ledesma, R. M., & Zenteno-Morán, D. (2019). Heat flow and geothermal provinces in Mexico. *Geothermics, 78*, 183–200.

Raymond, J., Williams-Jones, A. E., & Clark, J. R. (2005). Mineralization associated with scale and altered rock and pipe fragments

from the Berlin geothermal field, El Salvador; implications for metal transport in natural systems. *J. Volcanol. Geothermal Res., 145*, 81–96.

Reyes, A. G. (1990). Petrology of Philippine geothermal systems and the application of alteration mineralogy to their assessment. *Journal of Volcanology and Geothermal Research, 43*, 279–309.

Reyes, A. G. (1992). Petrology and fluid chemistry of magmatic-hydrothermal systems in the Philippines. In Y. K. Kharaka, and A. Maest (Eds.), *Proceedings of the International Symposium on Water-Rock Interaction* (Vol.7, pp. 1341–1344). A.A. Balkema.

Rodríguez, R., Armienta, M. A., Morales, P., Silva, T., & Hernández, H. (2006). *Evaluación de Vulnerabilidad Acuífera del valle de Irapuato, Gto*. Technical Report inedit. JAPAMI, CONACyTEG, IGF UNAM, México D.F.

Rodríguez-Díaz, A. A., Canet, C., Villanueva-Estrada, R. E., Chacón, E., Gervilla, F., Velasco-Tapia, F., Cruz-Gámez, E. M., González-Partida, E., Casas-García, R., Linares-López, C., & Pérez-Zárate, D. (2019). Recent Mn-Ag deposits in coastal hydrothermal springs in the Baja California Peninsula, Mexico. *Mineralium Deposita, 54*, 849–866.

Ronoh, I. (2015). *Appraising a geothermal field using hydrothermal alteration mineralogy: A case study of the East of Olkaria Domes Geothermal Field; Olkaria, Keny*a. World Geothermal Congress, Melbourne, Australia, 19–25 April.

Rosas-Elguera, J., & Urrutia-Fucugauchi, J. (1998). Tectonic control of the volcano-sedimentary sequence of the Chapala Graben, western Mexico. *International Geology Review, 40*, 350–362.

Rouwet, D. (2006). *Estudio geoquímico comparativo de los sistemas hidrotermales de los volcanes activos en Chiapas: El Chichón y Tacaná*. Ph.D. Dissertation, IGF–UNAM, p. 218.

Rye, R. O. (2005). A review of the stable-isotope geochemistry of sulfate minerals in selected igneous environments and related hydrothermal systems. *Chemical Geology, 215*, 5–36.

Sánchez-Córdova, M. M., Canet, C., Rodríguez-Díaz, A., González-Partida, E., & Linares-López, C. (2020). Water-rock interactions in the Acoculco geothermal system, eastern Mexico: Insights from paragenesis and elemental mass-balance. *Geochemistry, 80*, 125527.

Scheiber, J., Nitschke, F., Seibt, A., & Genter, A. (2012). *Geochemical and mineralogical monitoring of the geothermal power plant in Soultz-sous-Forêts (France)* (pp. 1033–1044). Stanford University.

Seal, R. R., II. (2006). Sulfur isotope geochemistry of sulfide minerals. *Review in Mineralogy and Geochemistry, 61*(1), 633–677.

Seal II, R.R., Alpers, C.N., Rye, R.O., (2000). Stable isotopes systematics of sulfate minerals. In: In: Alpers, C.N., Jambor, J.L., Nordstrom, D.K. (Eds.) Sulfate Minerals-Crystallography, Geochemistry, and Environmental Significance. Rev. Mineral, pp. 179–226

Sosa-Ceballos, G., Macías, J. L., Avellán, D. R., Salazar-Hermenegildo, N., Boijseauneau-López, M. E., & Pérez-Orozco, J. D. (2018). The Acoculco Caldera Complex magmas: Genesis, evolution and relation with the Acoculco geothermal system. *Journal of Volcanology and Geothermal Research, 358*, 288–306.

Spectral International Inc. (1994). *SWIR spectral mineral identification system and spectral database SPECMINT* (Vol. II). Integrated Spectronics.

Spycher, N. F., & Reed, M. H. (1989). As(III) and Sb(III) sulfide complexes—An evaluation of stoichiometry and stability from existing experimental data. *Geochimica et Cosmochimica Acta, 53*, 2185–2194.

Standard Methods for the Examination of Water and Wastewater. (2017). Baird, R. B., Eaton, A. D., Rice, E. W. (Eds.), *American Public Health Association, American Water Works Association and the Water Environmental Association* (23rd Ed.).

Strübel, G. (1967). Zur Kenntnis und genetischen Bedeutung des Systems $BaSO_4$-NaCl-H_2O. *Neues Jb Miner Monat* 223–234.

Taran, Y., Fischer, T. P., Pokrovsky, B., Sano, Y., Armienta, M. A., & Macias, J. L. (1998). Geochemistry of the volcano–hydrothermal system of El Chichón Volcano, Chiapas, Mexico. *Bulletin of Volcanology, 59*, 436–449.

Thompson, A.J.B., Thompson, F.J.H., (1996). Atlas of Alteration: A Field and Petrographic Guide to Hydrothermal Alteration Minerals. Geological Association of Canada, Mineral Deposits Division, 120 pp.

Torres-Alvarado, I. S. (2000). Mineral chemistry of hydrothermal silicates in Los Azufres geothermal field, Mexico. In *World Geothermal Congress, Kyushu-Tohoku, Japan, Proceedings: International Geothermal Association* (pp. 1861–1866).

Torres-Alvarado, I. S., Pandarinath, K., Verma, S. P., & Dulski, P. (2007). Mineralogical and geochemical effects due to hydrothermal alteration in the Los Azufres geothermal field, Mexico. *Revista Mexicana De Ciencias Geológicas, 24*, 15–24.

Tóth, J. (2005). Las aguas subterráneas como agente geológico: causas, procesos y manifestaciones. *Boletín Geológico. B. Geol. Minera, 111*(4), 9–26.

Venegas-Salgado, S., Herrera, J. J., & Maciel, E. R. (1985). Algunas características de la Faja Volcánica Mexicana y de sus recursos geotérmicos, *in*: S.R Verma (Editor), Special Volume on the Mexican Volcanic Belt-Part 1. *Geofísica Interncional, 24*(1), 47–81.

Verma, S. P., Torres-Sánchez, D., Velasco-Tapia, F., Subramanyam, K. S. V., Manikyamba, C., & Bhutani, R. (2016). Geochemistry and petrogenesis of extensión-realted magmas close to the volcanic front of the central part of the Trans-Mexican Volcanic Belt. *Journal of South American Earth Sciences, 72*, 126–136.

Villanueva-Estrada, R. E., Prol-Ledesma, R. M., Rodríguez-Díaz, A. A., Canet, C., & Armienta, M. A. (2013). Arsenic in hot springs of Bahía Concepción, Baja California Peninsula, México. *Chemical Geology, 48*, 27–36.

Wagner, T., Kirnbauer, T., Boyce, A. J., & Fallick, A. E. (2005). Barite-pyrite mineralization of the Wiesbaden thermal spring system, Germany: A 500-kyr record of geochemical evolution. *Geofluids, 5*, 124–139.

Web[1]. Retrieved April 13, 2020, from https://www.academia.edu/3987130/Alteraci%C3%B3n_Hidrotermal_1_ALTERACION_HIDROTERMAL.

Webster, J. G., & Nordstrom, D. K. (2003). Geothermal arsenic. In A. H. Welch & K. G. Stollenwerk (Eds.), *Arsenic in ground water: Geochemistry and occurrence* (pp. 101–125). Springer.

Wilson, N., Webster-Brown, J., & Brown, K. (2007). Controls on stibnite precipitation at two New Zealand geothermal power stations. *Geothermics, 36*, 330–347.

Yavuz, F., Gültekin, A. H., Örgün, Y., Çelik, N., Çelik-Karakaya, M., Karakaya, E., & Sasmaz, A. (2002). Mineral chemistry of barium and titanium bearing biotites in calcalkaline volcanic rocks from the Mezitler area (Balıkesir-Dursunbey), western Turkey. *Geochemical Journal, 36*, 563–580.

Younger, P. (2007). *Groundwater in the environment: An introduction* (pp. 74–92). Blackwell Publishing.

Journal:	**41513**
Article:	**173**

Author Query Form

Please ensure you fill out your response to the queries raised below and return this form along with your corrections

Dear Author

During the process of typesetting your article, the following queries have arisen. Please check your typeset proof carefully against the queries listed below and mark the necessary changes either directly on the proof/online grid or in the 'Author's response' area provided below

Query	Details Required	Author's Response
AQ1	Please confirm if the author names are presented accurately and in the correct sequence (given name, middle name/initial, family name). Author 1 Given name: [R. Rocha] Last name [Miller]. Also, kindly confirm the details in the metadata are correct.	
AQ2	Please check and confirm the hierarchy of all affiliations are correct and amend if necessary.	
AQ3	References Standard Methods for the Examination of Water and Wastewater (1995), Landa Arreguín et al. (2021) are cited in text but not provided in the reference list. Please provide references in the list or delete these citations.	
AQ4	Kindly check and confirm the equations are renumbered for sequential order.	
AQ5	Please check and confirm the inserted citation of Fig. 10 is correct. If not, please suggest an alternative citation. Please note that figures and tables should be cited in sequential order in the text.	